Politecnico di Torino

Politecnico di Torino

Master's Degree in Environmental and Land Engineering

A.a. 2023/2024

October 2024

Analysis of spatiotemporal patterns of snow cover and snowmelt floods in Austria using remote sensing data

Thesis advisors:

Alberto Viglione

Miriam Bertola

Candidate:

Riccardo Priola

Abstract

This study investigates the temporal dynamics of snow cover and its impact on flood events using MODIS snow cover data from Terra and Aqua satellites. The analysis has been conducted across the Danube River basin and Austria with a comprehensive dataset of snow cover and river discharges spanning from 2001 to 2021.

The MODIS sensors offer spatial resolutions of 500 meters and a daily temporal resolution, crucial for capturing snow cover variations. To address cloud obscuration, a specific threshold for cloud coverage has been chosen and merging techniques utilized to increase the accuracy of the snow cover data.

Our assessment reveals a general decreasing trend in snow cover across the Danube sub-catchments, with varying rates of decrease among different basins and elevation ranges. In particular, catchments with average high snow cover exhibited a steeper decline compared to those with lower snow presence. However, catchments at altitudes between 1800 and 2100 meters showed a more stable snow cover over time compared to those at lower elevations, such as 900 to 1200 meters.

For the Austrian study area, the analysis involved also 581 river measurement stations grouped across five different regions based on specific hydrogeological and climatic characteristics.

Focusing on winter and spring peak discharge values, this research uncovered significant regional variations, with spring peak discharge showing decreasing trends in the Southern and Northern Alpine regions, as well as across Austria. In contrast, increasing trends were identified in both annual and winter peak discharge.

The temporal evolution of snow cover in Austrian catchments was also analysed, revealing notable regional differences. The Southern Alpine region exhibited the smallest decline at -0.08, while the Northern Alpine region showed a more pronounced decrease of -0.36. The Mann-Kendall test was conducted across these regions to assess the significance of these monotonic trends, revealing significant results for the Northern Lowlands and Eastern Lowlands, but not for the previously mentioned Southern Alpine region.

The study underscores that snowmelt dynamics, including variations in snow cover, play complex roles in flood generation. Analysing the correlations between spring peak discharge and snow-covered area values from the week preceding the peak

across the five regions reveals that: in the Alpine region the correlation is negative, indicating an inverse relationship between snow/glacier melt and river discharge. This suggests that as the peak tends to increase, snow cover decreases. In contrast, the Southern Alpine region shows a slight positive correlation, which reflects the influence of Mediterranean storm systems interacting with snowmelt processes. The Northern Alpine and Northern Lowlands regions exhibit low correlations, suggesting that rainfall is a more dominant factor in influencing peak discharge than snow cover. Finally, the Eastern Lowlands display small positive correlations, which may be attributed to the effects of local convective storms and frontal systems on river discharge.

The results underscore the intricate relationship between snow cover and flood peaks. Satellite imagery provided a robust framework for analysing snow cover trends. Future research incorporating stochastic modelling could further clarify how projected climate changes might alter snow dynamics, particularly through shifts in snowmelt timing and snow elevation line.

Table of Contents

List of Figures

List of tables

1 Introduction

1.1 Drivers of floods in Europe

In Europe there are three parameters, so called “drivers”, that mainly govern the occurrence of floods: extreme precipitation, antecedent soil moisture and snowmelt. The significance of this processes responsible for flood generation varies across different regions of our continent, reflecting the diverse climatic and geographical conditions that influence how and where floods occur. Stratiform rainfall plays a meaningful role in regions like the Alps and the Carpathians, soil moisture surplus is particularly impactful in the Atlantic climate of Western Europe, whereas snowmelt is a key factor in the north-eastern areas. Additionally, rain-on-snow events hold some importance in the mid-mountain ranges of central Europe (Kemter et al., 2020).

Over the past few decades, specifically between 1960 and 2010, the relevance of flood generation processes has changed across different parts of Europe (Hundecha et al., 2020; Kemter et al., 2020).

Stratiform rainfall has become less significant in the northern regions but has gained importance along the Mediterranean coast. Soil moisture excess has become more relevant in the British Isles and in central and northern Europe. Snowmelt, dominant process in Eastern Europe, has seen a decline in its influence there. Rain-on-snow events have become less prominent in Western Europe, while their relevance has grown in some areas of Eastern Europe (Figure 1.1).

As a result of this shifts in the ruling flood types, the overall flood hazard results to be mutated.

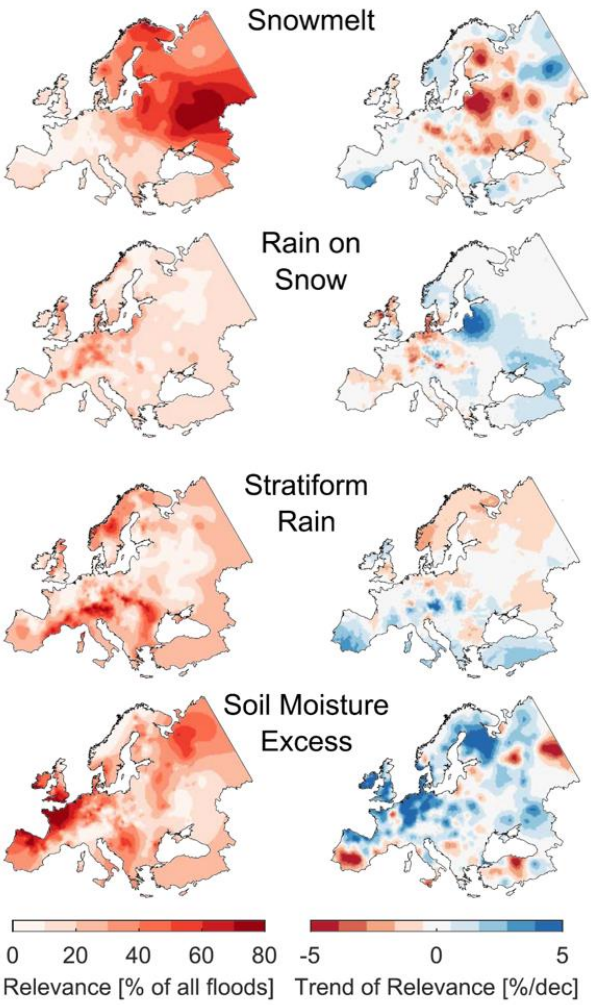

Figure 1.1: Significance of flood generating processes and corresponding trends from 1960 to 2010. Left: relevance of each process (quantified by the relative frequency of floods caused by that process). Right: trends of the annual relevance (change of the mean relevance per decade in percent) (Kemter et al., 2020)

The processes of snowmelt and rain-on-snow play a critical role in determining the occurrence and intensity of floods in temperate and cold regions of Europe, both at individual and seasonal extent. The likelihood of these processes leading to major flooding events is influenced by several variables, like the timing and synchronization of their components. Understanding these factors is challenging especially with rain-on-snow floods, yet it is essential for making more accurate flood hazard assessments.

1.2 Regional variations in snowmelt-induced floods

Regions in Europe where floods are ruled by snow have experienced notable shifts in the average occurrence and intensity of annual peaks over the last decades. Consequently, changes in flood risk have been linked to alterations in snowmelt and rain-on-snow processes (Blöschl et al., 2017, 2019b; Bertola et al., 2021). However, the specific causes behind these variations for each flood type and their combined impact on the overall flood risk at the catchment level are still not well understood. This is particularly true for rain-on-snow floods, which remain poorly studied yet have the potential to significantly heighten future flood risks (Haleakala et al., 2023).

In European regions where snowmelt is the primary factor driving floods, a decline in spring and summer snow cover has been observed in the last years and attributed to the global rising of temperatures. Research studies have shown a trend of reduced extreme streamflow and earlier peak flows during spring in these areas and that such snowmelt-induced floods are seldom extremely severe due to the limited amount of solar energy available for melting the snow (Merz and Blöschl, 2008; Madsen et al., 2014).

That said, it's important to underline that the effect of higher temperature is different in relation to the considered region. Two contrasting examples can be the northeastern side of Europe, where snowmelt is the main flood-generating process and where a decrease in melting can lead to a relevant mutation in the flood frequency curve, and, for instance, a region in the south part of Austria, called Carinthia, where the greater part of floods take place in autumn. Considering that spring snowmelt contribute to smaller events, a change in snow cover in this last region is likely to have a minor effect and just on lower magnitude floods (Merz and Blöschl, 2003).

1.3 Snow behaviour at the catchment scale

Flooding from snowmelt happens in areas covered by snow where a significant volume of water is retained within the snowpack. This melting process is triggered by a quick rise in air temperatures, typically over a span of one to two weeks. This results in soil saturation, increase in water flow and eventually leads to flooding.

To understand the behaviour of rain-on-snow floods is important to know that snow dynamics of the snowpack already present play a crucial role, in particular the thermal state influences the delay or retention of water.

Runoff is in fact affected by how much rainwater and meltwater infiltrate and exit the snowpack itself (Hirashima et al., 2017). Conversely, there can be areas within a catchment without snow which react in a different way to rain and melting. This combination leads to an overall more complex analysis regarding the timing and magnitude of runoff generation processes (Coles and McDonnell, 2018).
During events where rain falls on existing snow, the snowpack can impact runoff generation in different ways. It might absorb a substantial amount of water, thus reducing the risk of flooding, or it might increase runoff by causing additional snowmelt and a higher runoff rate. Anyway, this kind of events are affected by the distribution of snow cover, snow depth and rainfall within the catchment area, which vary based on time of year and altitude (Gravelmann et al., 2015).
Mid-elevation areas within a catchment, where the snowpack is relatively shallow, are typically the primary sources of runoff. Rainfall in these regions can easily melt the snow, leading to significant runoff even from moderate amounts of rain. During major events, the combination of rain and snow accelerates the snowmelt process. Additionally, previous snowmelt can raise the runoff rate by causing widespread saturation across the catchment area (Cohen et al., 2015; Merz and Blöschl, 2003).

Regarding the scale of interest, snowmelt and rain-on-snow processes are well known at small scale, from a single point to a hillslope, for example. However, their combined effect on a larger scale, like a catchment, and their impact on future climate change are two aspects that are still unclear (Haleakala et al., 2023).
It has been observed that since 1961 some characteristics of the snow such as amount of fresh snow, depth and duration of the snow cover are changed in a negative way in some regions of south-west Austria. The three factors responsible for an increase or a decrease in the amount of snow are: elevation, precipitation and air temperature. A change in the last two elements lead to different effects on snow and elevation influences the correlation between average winter snow depth and both air temperature and precipitation. Therefore, contrasting impacts on snow behaviour of air temperature and precipitation are consequently related to variation in runoff.
In Figure 1.2 it is shown that in some Austrian and Swiss stations has been observed that low-altitude stations show a strong sensitivity to temperature changes, whereas high-altitude ones are more affected by precipitation (Schöner et al., 2016).

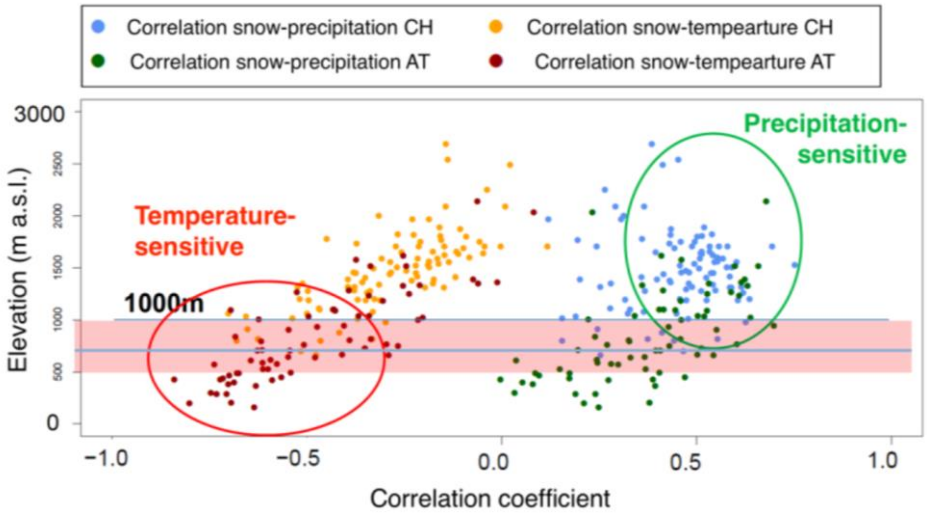

Figure 1.2: Correlation of snow depth in December, January and February with air temperature and precipitation as function of elevation in Austrian and Swiss stations (modified from Schöner et al., 2016)

1.4 The use of satellite

To examine snow cover characteristics during specific flood events, focusing on factors like snow cover extent and duration, to evaluate their temporal changes and to try to identify snowmelt induced floods, this project relies on high-resolution satellite images taken from remote sensing instruments.

The reason for this choice is based on the desire to provide a new perspective on the analysis of snow cover and melting processes. In fact, the latter two points are usually detected through: snow tracking stations (Garvelmann et al., 2015), hydrologic models recreating snow accumulation and melting processes (Merz and Blöschl, 2003; Hundecha et al., 2020) and reanalysis land-surface data (Cohen at al., 2015). Nevertheless, these techniques encounter several limitations primarily due to the restricted availability of direct measurements of snow and the uncertainties associated with various modelling approaches used to simulate snow dynamics. These constraints can affect the accuracy and reliability of the results obtained from these methods (Haleakala et al., 2023).

On the other hand, with satellite images we can effectively and precisely assess the extent of snow cover areas over large geographic regions (Parajka and Blöschl, 2012). MODIS (Moderate Resolution Imaging Spectroradiometer) provide remote sensing observations covering areas across the globe with a daily base and a high spatial resolution of 500 meters, combined with their extensive observation history spanning over 20 years. This level of detail allows for a thorough examination of

localized snow cover patterns within individual catchments and their influence on flood generation.

Although MODIS has proven effective in mapping snow cover and its seasonal changes (e.g. Paudel and Andersen, 2011; Wang et al, 2015), there are only a few studies that explore the use of MODIS for identifying and characterizing snow-driven floods and their variations.

In fact, a large portion of the research primarily examine the effects of rainfall and snowmelt together leading to a certain potential to causing flooding. However, these studies often do not extend to the analysis of real flood events using runoff data.

Cloud cover is one of the primary challenges in utilizing optical remote sensing products, as it makes detecting snow coverage difficult. However, this challenge can be addressed through several established methods that rely on filtering and snow mapping, which have proven effective in minimizing cloud interference (see chapter 2.3).

2 MODIS overview: background

To classify and characterize snow-driven floods on a large scale, high-resolution satellite data from optical sensors are employed to examine the within-catchment snow cover patterns, track their changes over the years and their behaviour before flooding events. In addition, we also rely on actual floods observation, registered from local measuring stations localized in our area of interest, to enhance the understanding of the processes responsible for the observed floods.
This approach is chosen to more effectively evaluate and understand the behaviour of snowmelt floods and it has been preferred to the majority of previous research methods that often relied on reanalysis data or model simulations for classifying snow-driven floods or use satellite data to assess the flood potential without incorporating actual flood observations.

2.1 MODIS

Monitoring snow accumulation and melt in mountainous regions is particularly challenging due to the relevant spatial variability of snow characteristics and the often limited availability of ground-based hydrological data. In such contexts, satellite imagery serves as a valuable alternative, as their resolution and availability are not significantly influenced by terrain features.
The MODIS (Moderate Resolution Imaging Spectroradiometer) sensor, mounted on NASA's Terra and Aqua satellites, has been widely used for snow cover monitoring. MODIS is an imaging spectroradiometer that employs a cross-track scan mirror, collecting optics, and a set of individual detector elements to provide imagery of the Earth's surface and clouds in 36 discrete, narrow spectral bands ranging from approximately 0.4 to 14.4 μm (Barnes et al., 1998). With a daily temporal resolution and a spatial resolution of about 500 meters, MODIS data represent a crucial resource for hydrological analysis. They are particularly suitable for large-scale

snow mapping (Hall and Riggs, 2007; Parajka and Blöschl, 2006) especially in mountainous areas where ground-based data are often scarce (Parajka et al., 2012; Parajka and Blöschl, 2008).

2.2 MODIS version 6.1 and NDSI threshold

The MOD10A1 and MYD10A1 datasets, which are part of the MODIS (Moderate Resolution Imaging Spectroradiometer) Collection 6.1 products, provide detailed information about snow cover through the Normalized Difference Snow Index (NDSI). This index is calculated by comparing the difference in reflectance between the visible spectrum (band 4) and the shortwave infrared spectrum (band 6), using the formula:

$$NDSI = \frac{band\ 4 - band\ 6}{band\ 4 + band\ 6}$$

Unlike earlier versions that provided only binary information about the presence or absence of snow, the NDSI values in the current MODIS products allow for more nuanced and accurate snow cover mapping. Numerous studies have demonstrated that the overall accuracy of MODIS during clear sky conditions typically falls within the range of 85–99%. This accuracy varies depending on factors such as land cover (Hall and Riggs, 2007), season (Parajka and Blöschl, 2006), snow cover persistency and snow depth.

Further investigation into the NDSI thresholds for snow cover mapping was conducted by Tong et al. (2020), who compared various thresholds against the traditional fixed NDSI threshold of 0.4. Their study, which involved daily snow depth observations from 665 climate stations across Austria from 2002 to 2014, revealed that the overall classification accuracy of MODIS snow cover products exceeded 97% (97.4% for Terra and 97.6% for Aqua) in Austria. The research also found that the best NDSI thresholds (BT_{NDSI}) varied depending on snow depth thresholds (TSD), with the median BT_{NDSI} at 665 stations ranging from 0.34 (for TSD = 1 cm) to 0.45 (for TSD = 5 cm) for Terra, and from 0.37 (for TSD = 1 cm) to 0.45 (for TSD = 5 cm) for the Aqua daily dataset (Figure 2.1).

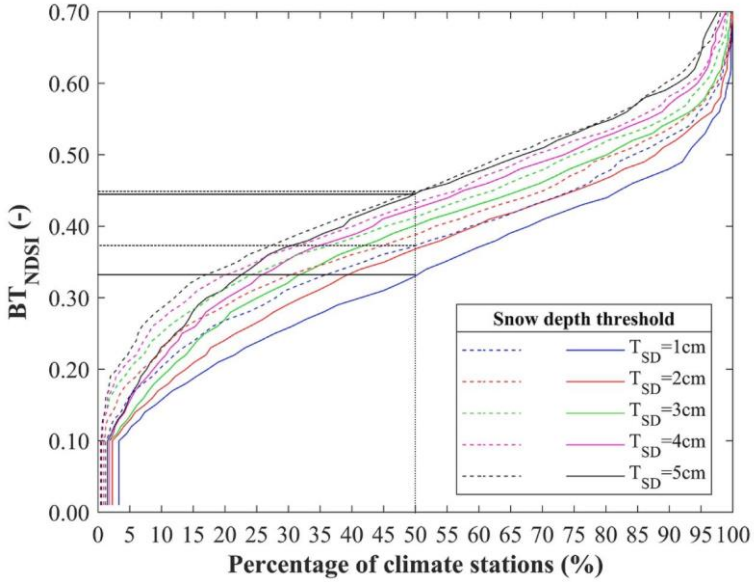

Figure 2.1: Cumulative distribution functions of the best NDSI threshold (BTNDSI) determined for Aqua (dashed line) and Terra (solid line) snow cover products, using various snow depth thresholds (1 cm, 2 cm, 3 cm, 4 cm, and 5 cm) at 665 stations from September 2002 to August 2014 (modified from Tong et al. (2020))

The study also highlighted that NDSI thresholds are not static but vary seasonally, decrease with increasing elevation, and are lower in forested areas compared to open land. Adjusting NDSI thresholds to account for different elevation and land cover classes was shown to improve regional snow cover mapping accuracy by 3-10% in forested regions above 900 m a.s.l. during the months of January to March. Given these findings, as final consideration, Tong et al. (2020) suggested that the traditional NDSI threshold of 0.4 remains robust for snow cover mapping applications in regions with similar physiographic conditions to those studied.

2.3 MODIS satellite image merging and cloud cover threshold

Cloud cover has been identified as a significant challenge in applying MODIS snow cover products, particularly in regions like Austria where the average cloud coverage reached 63% between 2000 and 2005 (Parajka and Blöschl, 2006). This issue becomes even more pronounced during the winter months, a critical period for snow cover analysis. To address this, Parajka and Blöschl (2008) proposed a method to reduce cloud coverage by merging the MODIS snow cover data from the Terra and Aqua satellites, which capture observations just a few hours apart.

Their research demonstrated that this approach is highly effective, yielding snow maps that maintain strong agreement with ground-based snow observations.
In their study, Parajka and Blöschl (2008) introduced three distinct approaches to combine the Terra (T) and Aqua (A) MODIS products.
The first method, known as the combination (CM) approach, merges snow cover data on a pixel-by-pixel basis. If a pixel is classified as cloud-covered in the Aqua image, it is updated with the corresponding Terra pixel value if the latter indicates snow or land. This method effectively combines observations from the same day, separated by only a few hours.
The second approach, termed the spatial filter (SF), involves replacing cloud-covered pixels with the most common land or snow class found among the eight surrounding non-cloud pixels. This spatial filtering is applied to the combined Terra-Aqua images generated by the first method.
The third approach, known as the temporal filter (D), replaces cloud-covered pixels with the most recent non-cloud observation at the same location within a set temporal window of 1, 3, 5, or 7 days. Similar to the SF approach, this method is also applied to the combined Terra-Aqua data from the first method.
The snow-covered area (SCA) is calculated as the ratio of snow pixels (S) to the total number of snow and land pixels (S + L) for each zone on a given day:

$$SCA = \frac{S}{S + L}$$

The area occupied by clouds is calculated as the ratio of cloud pixels (C) to the total number pixel given as the sum of cloud, land and snow (C + S + L) for each zone on a given day:

$$CLOUD = \frac{C}{C + S + L}$$

Since the accuracy and reliability of SCA estimates depend also on the extent of cloud coverage, in Figure 2.2 it's represented the seasonal distribution of cloud coverage and the effect of merging Terra and Aqua over Austria for the period 2003–2005. Aqua has marginally higher cloud coverage than Terra and combining the two results in a significant reduction in cloud coverage.
Combining the two snow cover products on the same day lowers cloud coverage by around 4% in February for Terra and over 21% in August for Aqua. This merging of

Aqua and Terra snow cover images was performed on a pixel basis, so using the so-called combination approach.

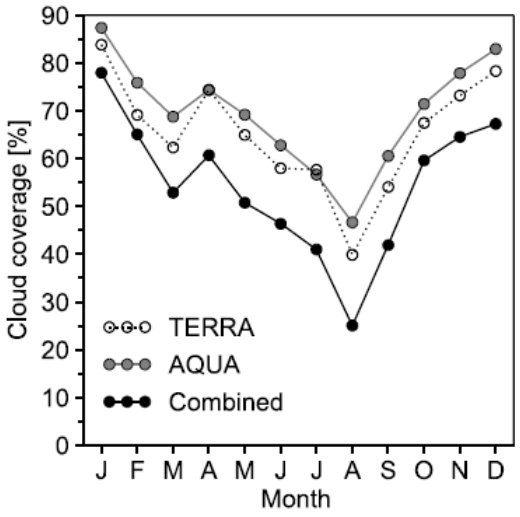

Figure 2.2: Median daily cloud coverage of Terra, Aqua, and combined Terra-Aqua MODIS snow maps across Austria for each month during the period 2003-2005 (Parajka and Blöschl (2008))

As example, Figure 2.3 displays the two images acquired from Aqua and Terra satellites, together with the result of the merging process for a random day within the defined period.

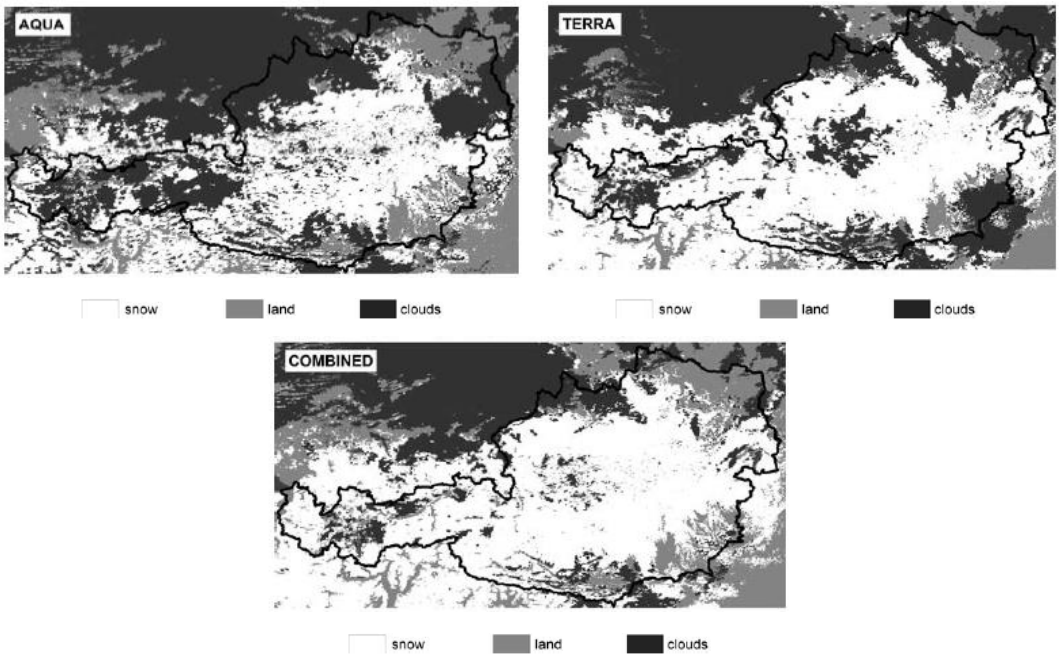

Figure 2.3: Austria snow cover images the 25th of October 2003. Top left: Aqua. Top right: Terra. Bottom central: Result of the merging of Aqua and Terra (modified from Parajka and Blöschl (2008))

To manage the cloud coverage problem, Parajka and Blöschl (2008) defined a cloud cover threshold, ξ_c, above which SCA estimates would not be considered reliable for analysis. The selection of ξ_c involves a trade-off between the availability of MODIS images and the reliability of SCA estimates; as the cloud cover threshold increases, more images become available, but the accuracy may decrease.
This is shown in Figure 2.4 in terms of the percentage of number of days that are available for SCA estimation considering the different presented merging techniques.

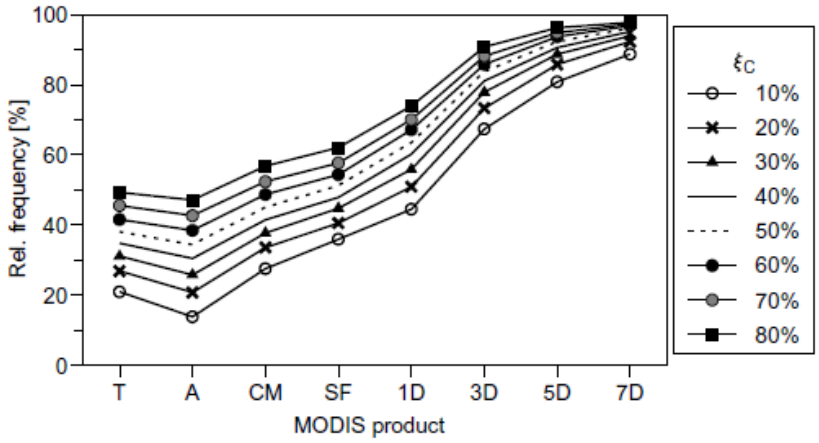

Figure 2.4: Frequency of days available for calculating snow cover area (SCA) from MODIS, across various cloud thresholds ξ_c ranging from 0.10 to 0.80, expressed relative to the total number of days during the 2003-2005 period. Median values are evaluated over 148 selected catchments (Parajka and Blöschl (2008))

Figure 2.4 shows that, for instance, when using the combined Terra/Aqua product (CM) and setting the threshold ξ_c at 20%, SCA images were available on at least 33% of days in half of the catchments. As the threshold ξ_c increases, so does the availability of SCA images. The availability also improves when transitioning from individual Terra/Aqua images to their combined products.
An example of SCA estimation is provided for an Austrian catchment, the so-called "Obertraun" (Figure 2.5), where there are compared two different scenarios: catchment with less than 10% cloud cover (ξ_c = 10%, top panel) and with a 60% cloud threshold (ξ_c = 60%, bottom panel).

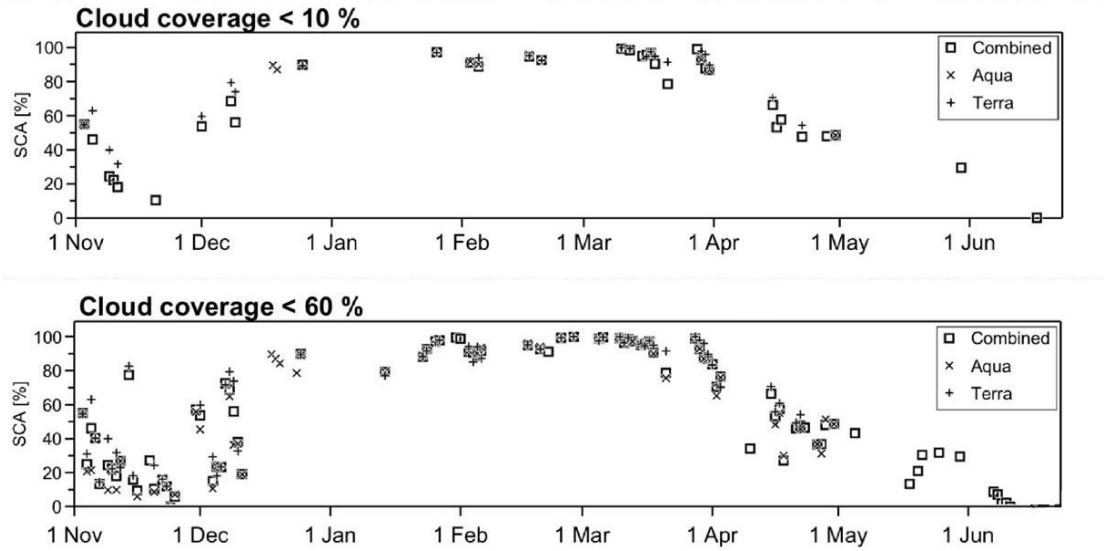

Figure 2.5: MODIS snow cover area (SCA) estimation in the Obertraun catchment during the 2004 snow season. SCA is calculated considering images with less than 10% (ξc=10%, top panel) cloud cover and 60% (ξc=60%, bottom panel) cloud cover (modified from Parajka and Blöschl (2008))

The SCA estimates from the original Aqua and Terra products, as well as their combination (CM), showed that a less restrictive cloud criterion (ξ_c = 60%) allowed for more frequent SCA estimates. Despite the higher threshold, the estimates remained robust, with only minor differences observed in early December and April due to, probably, more frequent snowmelt and rain-on-snow events.

3 Study sites

3.1 Danube River basin

The study is focused on two distinct areas. A first initial analysis is done for a very large region encompassing all the catchments of the Danube River. This area is subdivided into 104 catchments, ranging from 97 to almost 800000 km^2 with an average of 67065 km^2 (Figure 3.1). We extract information about the type of land cover detected in each catchment using satellite imagery for a reference time series.

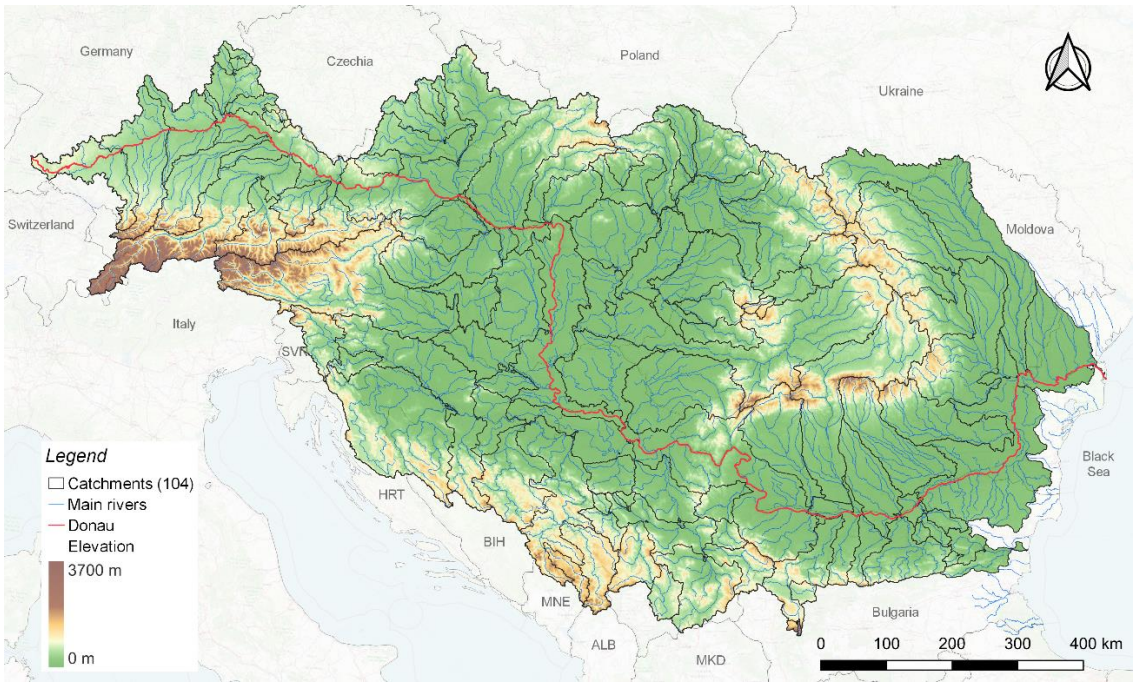

Figure 3.1: Study site number one: Digital Elevation Model of the Danube River area divided in 104 sub-catchments from its source to its mouth

3.2 Austria

To deepen the study, it has been chosen a second more strict area where the amount of available data is richer. This selected area corresponds to the state of Austria. In particular we focus our attention on the catchments which have a streamflow measuring station located in Austria. Among the 943 available stations we excluded the ones on the border with other countries with the related catchments mainly spreading in regions outside Austria and also those assessing catchment areas larger than 10000 km^2 because of a too big extension, that is synonymous of not being enough representative of the local environment. In the end we selected a total of 909 stations, with catchments ranging from a few km^2 to a maximum of 10000 km^2.

As detailed in the data chapter, all these stations provide us with annual peak flow data. However, for our case study this is not enough, as we also require daily flow data to evaluate peak discharge during the winter and spring months. Among these stations, 581 provide daily flow values, and consequently, these are the stations we have referenced and used.

They were then subdivided in five regions according to different hydrological processes, climatic conditions and flood generating mechanisms: alpine, southern alpine, northern alpine, northern lowlands and eastern lowlands (Merz and Blöschl, 2009).

Table 1 presents the number of stations considered for each region, along with the total count distributed across the country (Figure 3.2).

Regions	Number of considered stations
Alpine	92
Southern alpine	112
Northern alpine	139
Northern lowlands	143
Eastern lowlands	95
Total	581

Table 1: Subdivision of the 581 considered Austrian stations in five specific regions according to different hydrological conditions, as in Merz and Blöschl, 2009

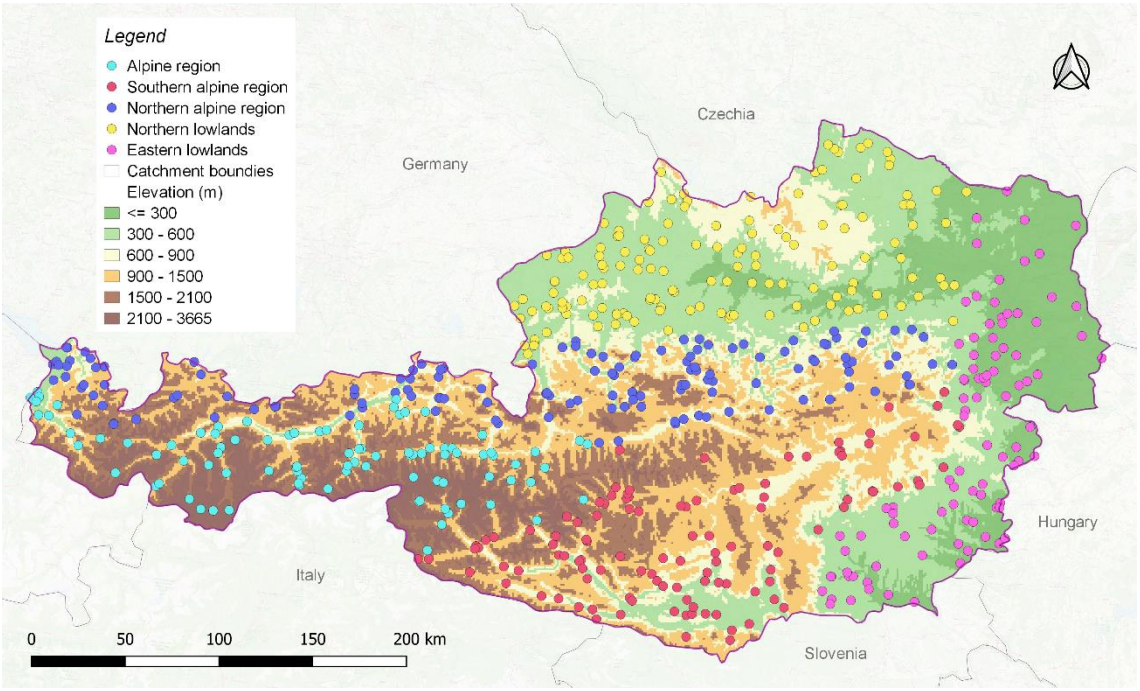

Figure 3.2: Study site number two: Digital Elevation Model of Austria and location of the evaluated measuring stations, subdivided in five different hydrological regions, as in Merz and Blöschl, 2009

In Table 2 are showed the characteristics in terms of area and elevation of the catchments evaluated by our stations. For each region the table highlights the catchment area of the smallest and largest basin, as well as the average value for all basins within the region. Similarly, it presents the elevation of the lowest and highest basins, followed by the regional average.

Regions	*Area (km^2)*			*Elevation (m)*		
	min	max	avg	min	max	avg
Alpine	9.2	5772	545	419	2640	992
Southern alpine	9.3	6792	620	354	1995	675
Northern alpine	3.9	9310	470	325	1454	605
Northern lowlands	10.6	6120	408	185	722	389
Eastern lowlands	11.6	7043	420	122	408	257

Table 2: Minimum, maximum, average area (in km^2) and outlet elevation (in m) of our considered Austrian stations divided in the five defined regions, as in Merz and Blöschl, 2009

Austria exhibits a wide range of hydrological conditions, from the eastern lowlands with average elevations below 200 meters, to the high alpine regions in the west, where elevations exceed 2500 meters. Annual precipitation also varies significantly, with less than 400 mm per year in the east and over 3000 mm per year in the west, largely due to orographic influences that increase rainfall (Merz and Blöschl, 2009).

The "alpine region" in western Austria, encompassing the Alps, is notably influenced by snow and glacier melt, which play a crucial role in runoff generation. Streamflow and flooding in this area are notably affected by these melt processes. Most floods occur during the summer, primarily due to frontal weather systems, sometimes combined with local convective storms. Early summer floods are often preceded by snowmelt, which increases soil moisture levels, contributing to the severity of flooding.

The "southern alpine region" of Austria, encompassing alpine catchments in East Tyrol and along the river Gail, shares hydrological similarities with the alpine region. However, Mediterranean storm tracks play an influential role, heavily influencing soil moisture variability. In the lower parts of this region, particularly southeast of the Alps, rainfall is notably lower, and snow processes have a reduced impact. While snowmelt-driven floods are common in May, the most severe floods occur in autumn, driven by Mediterranean storm systems.

The "northern alpine region" lies along the northern edge of the central Alps and experiences the highest rainfall in Austria, largely due to the orographic effects of the Alps on north-westerly airflows. In this area, significant rainfall occurs, leading

to frequent summer floods primarily driven by frontal weather patterns, with minimal influence from snowmelt.

The "northern lowlands" are characterized by relatively flat terrain and receive less rainfall compared to the northern alpine region due to a reduced orographic effect. Floods in this area can occur in both summer and winter. Winter floods are often triggered by rain-on-snow events, where prior snowmelt saturates the soil, making even low-intensity rainfall capable of causing considerable flooding.

The “eastern lowlands”, situated in the east and northeast, are the driest region in the country. Characterized by a continental climate, this area experiences warm, dry summers and cold winters with minimal snowfall. The region's flat catchments typically receive low annual rainfall, with floods occurring primarily in the summer due to frontal systems, occasionally intensified by local convective storms (Gaál et al., 2012; Merz and Blöschl, 2009).

4 Data and methods

4.1 MODIS data

The MODIS data integrated into this study are derived from observations acquired by the MODIS optical instruments on the Terra and Aqua satellites of NASA's Earth Observation System. These observations are available as global snow cover products through the Data Access Tool at the National Snow and Ice Data Centre (NSIDC). The NSIDC provides detailed technical documents that describe the snow mapping algorithm, data formats, spatial and temporal resolutions, and references to validation studies.

This analysis utilizes MODIS data covering the period from February 24, 2000, to December 31, 2022. Both our fields of study are covered by the MODIS sinusoidal grid tiles h18v04, h19v03, h19v04, and h20v04.

For every pixel within these four tiles, we extracted information on land cover, distinguishing between snow-covered, non-snow-covered, and cloud-covered areas. We then retrieved pixel values for the region encompassing the 104 catchments contributing to the Danube River's flow, as well as for the basins analysed in Austria. Regarding the first survey area, the same information extraction is then performed across the same region, this time categorizing the different type of land cover according to elevation ranges, from sea level up to 3700 meters, with progressive increment of 300 meters.

This differentiation has the primary goal of analysing whether points within the same elevation range exhibit similar behaviour, regardless of differences in the local environment associated with their specific area of origin.

In accordance with the results showed by the study of Tong et al. (2020) presented in the chapter 2.2, to extract information from satellite imagery differentiating between land, snow and clouds we decided to adopt a fixed NDSI value of 0.4.

This approach ensures consistent and reliable snow cover estimates from MODIS (C6) datasets.

$$NDSI = \frac{band\ 4 - band\ 6}{band\ 4 + band\ 6} = 0.4$$

Once a value is obtained for each pixel, the Snow-Cover Area (SCA) and the Cloud-Cover Area are determined to every daily image from both the Terra and Aqua satellites.
SCA is obtained by dividing the number of snow pixels (S) by the sum of snow and land pixels (S + L):

$$SCA = \frac{S}{S + L}$$

The Cloud-Cover Area is evaluated by dividing the amount of cloud pixels (C) by the total number of pixels, given as the sum of cloud, land and snow (C + S + L):

$$CCA = \frac{C}{C + S + L}$$

Based on the results obtained from Parajka and Blöschl (2008) in their study showed in chapter 2.3, we considered as significant only the SCA values for which, in each basin, every day, the percentage of pixels identified as clouds was less than a defined threshold ξ_c of 60%. In cases where cloud cover exceeded 60%, a NA value was assigned for that day in that area.

Since MYD10A1 data from the Aqua satellite are available only from July 4, 2002, Terra satellite data (MOD10A1) were used exclusively until that date. Afterword, data from both satellites were merged for the analysis in order to decrease the presence of NA inside the database.
In this work we use the merging technique called combination (CM) but in the opposite way respect to Parajka and Blöschl (2008). Meaning that the pixels classified as clouds in the Terra images are updated by the Aqua pixel value of the same location if the Aqua pixel is evaluated as snow or land.

4.1.1 Example of data extraction for one day of case study n°1

Es example, we report the procedure necessary to obtain information about the land cover type for one random day: the 19th of April 2019.

The first step consists of reading and implement in R the needed maps (Digital Elevation Model and Boundaries of the area) before the processing of MODIS images.

The Danube boundary is obtained from ccm (Catchment Characterisation and Modelling) outline map present in the Joint Research Centre Data Catalogue website, considering that Danube is corresponding to the WINDOW ID "2005".

After a crop of the DEM to the Danube catchments boundaries we obtained a tif file of the DEM.

Then we proceed to read the four tiles of MODIS for the 19th of April 2019, for Terra satellite:

- MOD10A1.A2019092.h18v04.061.2020291102913,
- MOD10A1.A2019092.h19v03.061.2020291103845,
- MOD10A1.A2019092.h19v04.061.2020291103346,
- MOD10A1.A2019092.h20v04.061.2020291103347.

And for Aqua satellite:

- MYD10A1.A2019092.h18v04.061.2020291104849,
- MYD10A1.A2019092.h19v03.061.2020291105354,
- MYD10A1.A2019092.h19v04.061.2020291105357,
- MYD10A1.A2019092.h20v04.061.2020291105011.

We then did the resample (project) of the images to the DEM and the collection (mosaic) of the four maps (Figure 4.1):

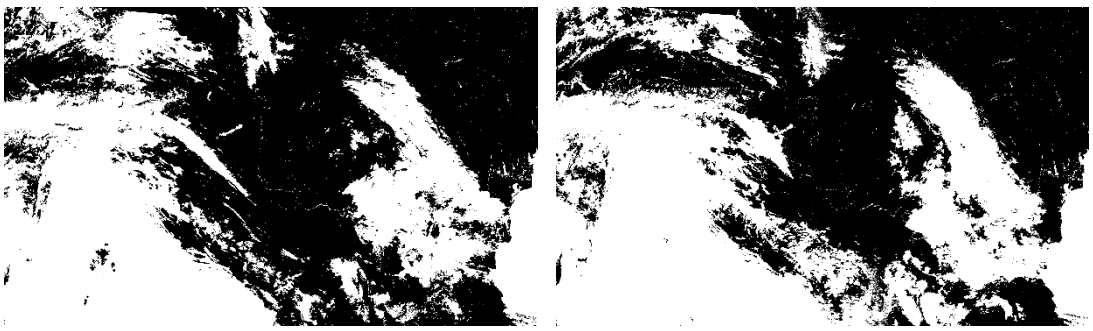

Figure 4.1: Terra (left) and Aqua (right) satellite images from MODIS the 19th of April 2019, sinusoidal grid tiles: h18v04, h19v03, h19v04 and h20v04

To obtain the needed information about land/snow/cloud cover for each pixel, we set the break values according to the threshold previously defined:

- NDSI < 0.4: detection of land,
- NDSI > 1: detection of cloud.

The pixel in between 0.4 and 1 were classified as snow.
Figure 4.2 shows the Terra and Aqua acquisitions with the pixels classified in one of the three different classes.

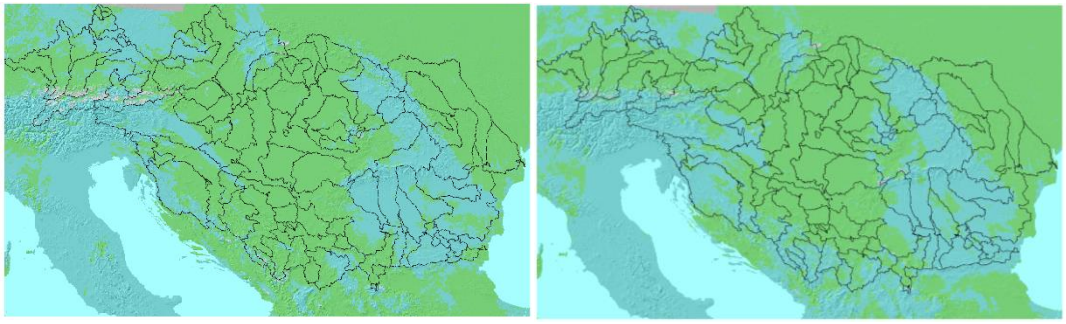

Figure 4.2: Terra (left) and Aqua (right) satellite images the 19th of April 2019, showing the classification of each pixel: land (green), snow (white) and clouds (light blue) base on the value of each cell

The extracted pixel frequencies showed the following distribution:

- Terra: land = 66.02%, snow = 1.55%, clouds = 32.43%,
- Aqua: land = 60.75%, snow = 0.58%, clouds = 38.67%.

The merging operation was than performed to reduce cloud cover, resulting in the following values: land= 75.19%, snow= 1.75%, clouds= 23.06%.
Pixel frequencies were then extracted for every catchment and range of elevations of our interest.

4.2 Runoff data

Streamflow data from rivers in our second region of interest, Austria, are incorporated into the analysis due to the availability of flow measurements from gauging stations distributed across the region. We use this data, provided from the eHYD ("Elektronische HYdrographische Daten") website with a daily temporal resolution, to examine river discharge behaviour over the past two decades and to identify any change.
The discharge data we have available extends until the end of 2021, but the start date of each time series varies from one station to another.

Table 3 lists, for each region, the average number of years for which data is available and the average start year of the data series in that region.

Regions	Average number of years in data series	Observation period
Alpine	53	1969-2021
Southern alpine	49	1973-2021
Northern alpine	49	1973-2021
Northern lowlands	47	1975-2021
Eastern lowlands	43	1979-2021
Total	48	1974-2021

Table 3: Number of years and interval time of availability of discharge data series for every Austrian region and, on average, for Austria

4.2.1 Specific discharge

For each region and for the entire country we evaluate the specific discharge. It is a hydrological measure that quantifies the rate of flow per unit area of a drainage basin. It is defined as the volume of water flowing per unit of time divided by the area of the catchment.

This metric helps to standardize flow measurements to account for variations in basin size, enabling comparisons between different catchments.

In mathematical terms it is expressed as:

$$Specific\ discharge = \frac{Q}{A}$$

Where:

- Q is the flow rate, in cubic meters per second (m^3/s),
- A is the area of the catchment, in square kilometre (km^2).

The unit of measure is the cubic meters per second per square kilometre ($m^3/s/km^2$).

Table 4 displays the average specific discharge in our regions of interest in the defined time period.

Regions	Specific discharge ($m^3/s/km^2$)
Alpine	0.0465
Southern alpine	0. 0457
Northern alpine	0.2157
Northern lowlands	0.1544
Eastern lowlands	0.0439
Total	0.1129

Table 4: Specific discharge in the five considered regions and averaged over all the Austrian stations

4.3 Peaks in runoff, SCA and chosen seasons

The very first part of the analysis of runoff data in Austria focuses on the temporal evolution of the annual maximum of discharge peaks.

Most yearly discharge peaks occur during summer, driven by intense precipitation events (Blöschl et al., 2017). Therefore, to better understand the role of snowmelt in contributing to high river discharge, we decided to focus our analysis on winter (December, January, February) and spring (March, April, May) maxima discharges. By examining the period leading up to these events, we track snow cover extent and its variations, both spatially and temporally, to assess its influence on discharge peaks.

The obtained datasets developed from the satellite' images provide detailed snow cover maps, which can be help characterize snowmelt processes and improve runoff predictions during snowmelt periods.

We focus on winter and spring because snowmelt processes during these seasons are more likely to impact river discharge, differently from annual discharge peaks, which are often driven by strong precipitation and may not reflect snowmelt contributions.

The analysis considers Snow-Covered Area (SCA) in three time windows prior to peak discharge: the seven days before the peak, the second-to-last week, and the third-to-last week. To estimate snowmelt's contribution to discharge, we calculate the difference between the average SCA in the second and third weeks and the last week before the peak, referred to as "Delta SCA".

4.4 Linear trend

To examine how discharge values and snow-covered areas have changed in time, the initial analysis focuses on the linear regression with time of data.
This operation is done in R through the command:

```
lm(dependent_variable ~ independent_variable, data = dataset)
```

The dependent variable is the data of interest in each case, while the independent variable is time. Data contains the specific dataset relevant to the study.
The lm function calculates the parameters (coefficients) that best fit the data by minimizing the sum of squared differences between the actual and predicted values, using the method of least squares.
After fitting the model, we obtain the coefficients that represent the estimated parameters of the linear model that best align with the data. We focus on the value of slope, which tells how much the dependent variable changes for every increase of one unit in the independent variable. Thus, it indicates the direction and strength of a trend. A positive slope shows an increasing trend, a negative slope reflects a decreasing trend and a slope of zero indicates a stable trend in time.

4.5 Mann Kendall test and Pearson Correlation

To determine the significance of the values obtained for snow cover time series, p-values is calculated using the Mann-Kendall test. It is a non-parametric test used to identify monotonic trends (increasing or decreasing) in time series data. This test provides the p-value for statistical significance. In R, the function `Kendall` is used to perform this evaluation.
A p-value threshold of 0.05 is used to determine statistical significance. If the p-value is below 0.05, the result is considered statistically significant, indicating strong evidence against the null hypothesis, and suggesting a meaningful monotonic trend in the data. Conversely, a p-value greater than 0.05 suggests that the observed trend is not statistically significant, implying insufficient evidence to reject the null hypothesis of no trend.

Pearson correlation and the corresponding p-value are calculated to assess the correlation between the magnitude of winter/spring flood peaks and snow cover in the preceding week, as well as the relationship between peak discharge and snowmelt between the second-to-last and last week before the flood event.

This method evaluates whether there is a statistically significant linear relationship between the variables. The p-value assesses the significance of the calculated correlation coefficient. In R, the p-value for Pearson's correlation coefficient can be calculated using the `cor.test()` function, that performs a correlation test and returns the associated p-value.

In R, the Pearson correlation coefficient between two sets of values is calculated using the following formula:

$$\rho = \frac{\sum_{i=1}^{n}(x_i - \bar{x})(y_i - \bar{y})}{\sqrt{\sum_{i=1}^{n}(x_i - \bar{x})^2}\sqrt{\sum_{i=1}^{n}(y_i - \bar{y})^2}}$$

Where x_i and y_i are the individual values of the two variables, $\bar{x}$ and $\bar{y}$ their means and n is the number of pairs of data points. This formula calculates the covariance between the two variables, normalized by the product of their standard deviations, to give a value between -1 and +1 that indicates the strength and direction of the linear relationship between the variables: ρ = +1 means perfect positive correlation, ρ = -1 a perfect negative correlation and ρ = 0 no relationship.

In paragraph 5.2.4 scatter plots are presented as a graphical tool for assessing the linear relationship between two quantitative variables. Each point on the scatter plot represents a pair of values, with the horizontal axis representing the independent variable, specifically the peak discharge values, and the vertical axis representing the dependent variable, in this case, the corresponding snow-covered area values. The position of each point in the plot reflects how one variable changes in relation to the other. This visual method allows for an intuitive examination of the correlation, providing insights into the strength and direction of the association between peak discharge and snow cover.

4.6 Boxplots

In paragraph 5.2.5, box plots are presented to highlight the differences among the Austrian regions. They are a kind of graph that are effective to visualize the distribution of a dataset, the middle point and the presence of any outliers.
In this analysis, box plots are employed to compare the correlation coefficients between regions with particular focus on the median values, at this phase of the research.

5 Results

5.1 Danube River basin

5.1.1 Temporal evolution of Snow-Covered Areas across different catchments

For each of the 104 sub-basins within the first study area, series of daily snow cover were estimated from MODIS daily images. From this, an annual mean value was calculated, representing the fraction of the sub-basin area that is covered by snow on average in one specific year. As an initial analysis, the trend over time of the annual mean snow cover was assessed using a linear coefficient to interpolate the temporal data. The results are shown in Figure 5.1.

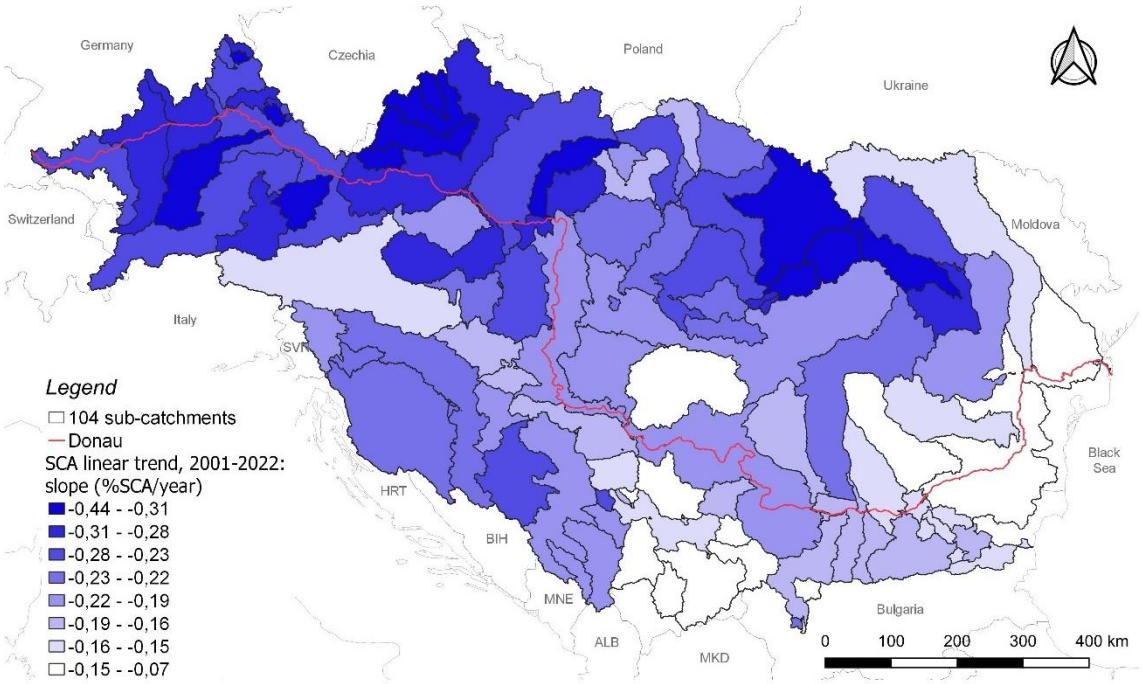

Figure 5.1: Trend of mean annual Snow-Covered Areas across the 104 sub-catchments contributing to the Danube River, for the period 2001 - 2022

Each basin is assigned to a colour indicating the slope value of the linear trend. It can be observed that the entire region exhibits a negative trend, indicating a decrease in snow cover. However, the trends vary significantly, ranging from a lower negative slope of 0.07 %/year to a maximum negative slope of 0.44 %/year.
Our available data period spans from the 24th of February 2000 to the end of 2022. However, since 2000 is missing data for January and much of February, which are critical months for the annual total SCA due to significant snow presence during winter, this year has not been included in the analysis. The incomplete data for 2000 would result in an inaccurate, unrealistically low SCA value compared to reality. Including 2000 would have flattened the slope of the interpolated line due to the incorrect lower value at the start of the series.
To understand the trend shown in Figure 5.1, we analysed four different catchments: two with a large negative slope (dark blue) and two with a smaller negative slope (white). The catchments are named Inn, Bistrita, Arges and Velika Morava, and are displayed in Figure 5.2.

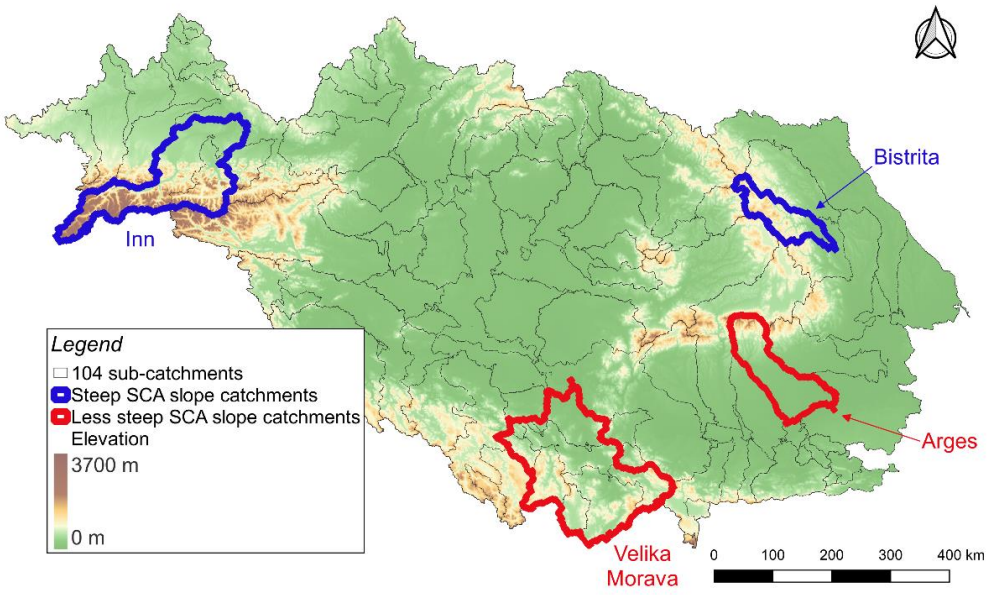

Figure 5.2: Focus on four interesting catchments with different behaviours. Inn and Bistrita basins, in blue, show a more negative SCA slope in time compared to Arges and Velika Morava, in red

It is immediately evident that the more negative trends in snow cover over time (in the blue-coloured catchments) are due to a generally higher average snow presence during the year. On the other hand, the red-identified catchments, because of their geographic location, experience lower average snow cover

throughout the year. This results in a slower rate of decline over time, making the decrease in snow cover less noticeable. The year-by-year snow cover values and their linear trends over time for these four selected catchments are shown in Figure 5.3. Table 5 provides, for each catchment, the snow cover values of the linear trend for the first and last year, as well as the difference between them. It is evident that a higher snow presence is associated to a more pronounced loss of snow over time.

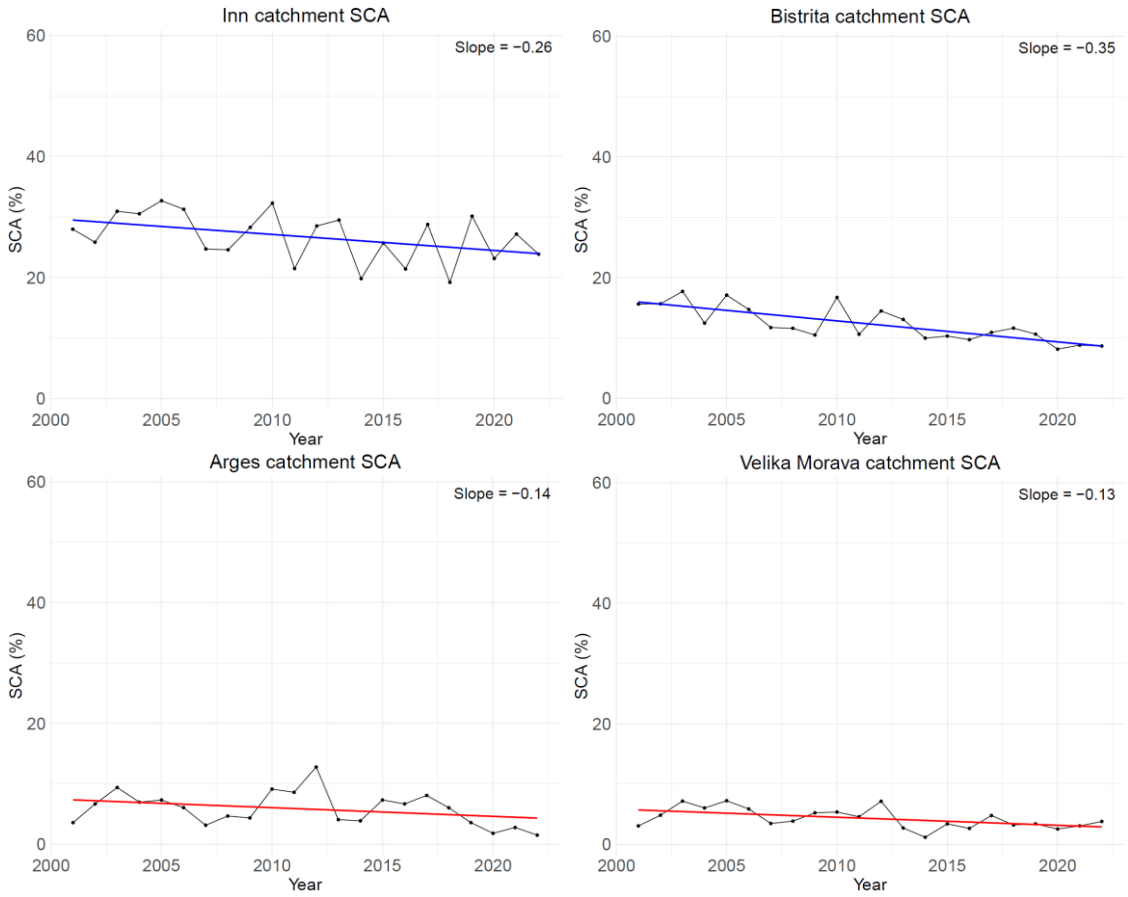

Figure 5.3: Average yearly SCA of the catchments: Inn and Bistrita (in blue), Arges and Velika Morava (in red)

Catchments	2001 SCA (%) from linear trend	2022 SCA (%) from linear trend	Difference (%) 2022 – 2001
Inn	29.48	23.93	- 5.55
Bistrita	15.94	8.63	- 7.31
Arges	7.32	4.30	- 3.02
Velika Morava	5.68	2.87	- 2.81

Table 5: Values of SCA from linear trend in 2001, 2002 and their difference, over the four considered catchments

5.1.2 Temporal evolution of Snow-Covered Areas across defined elevation ranges

Observing Figure 5.1 and Figure 5.2 together, and based on the findings for the Inn, Bistrita, Arges, and Velika Morava catchments, as well as public perception, one might conclude that catchments located at higher elevations predominantly exhibit a more negative slope in the interpolated line for the annual mean SCA values. Thus, the temporal evolution of SCA is analysed across different elevation ranges, from 0 to 3700 meters, with intermediate intervals of 300 meters (Figure 5.4).

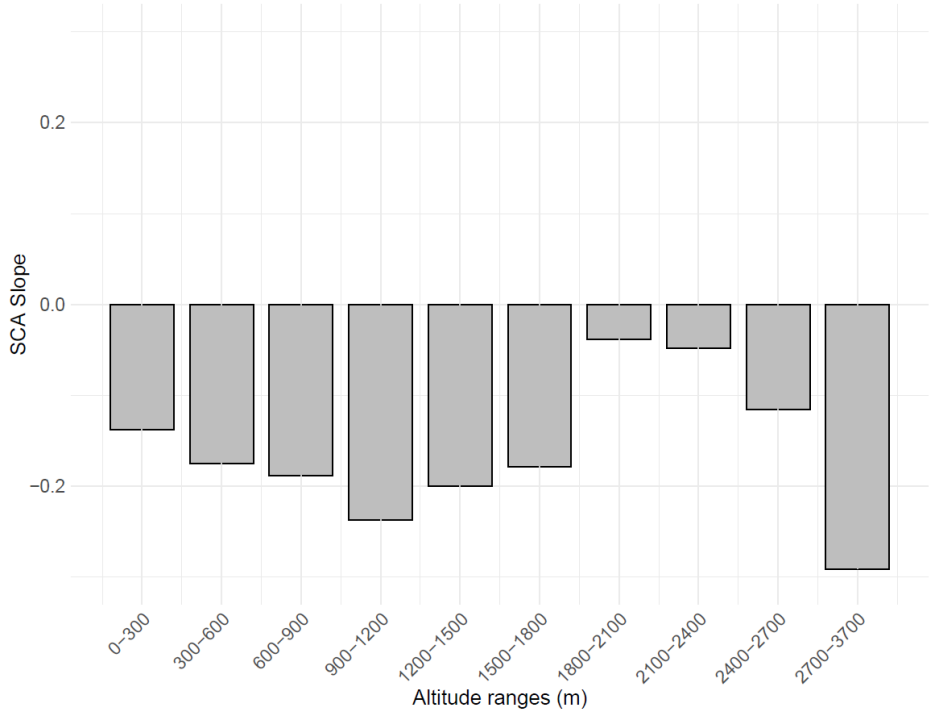

Figure 5.4: SCA slope of the interpolating line for different altitude ranges during the period 2001–2022 in the Danube catchment region

A decrease is observed across every possible elevation range, but it is very well appreciable that the trend differs from what was previously hypothesized. Specifically, the range between 1800 and 2400 meters shows a smaller decline in SCA compared to lower elevation ranges. Figure 5.5 illustrates the annual trends of snow cover for all areas in the Danube basin with elevations between 900 and 1200 meters (in red) and between 1800 and 2100 meters (in blue).

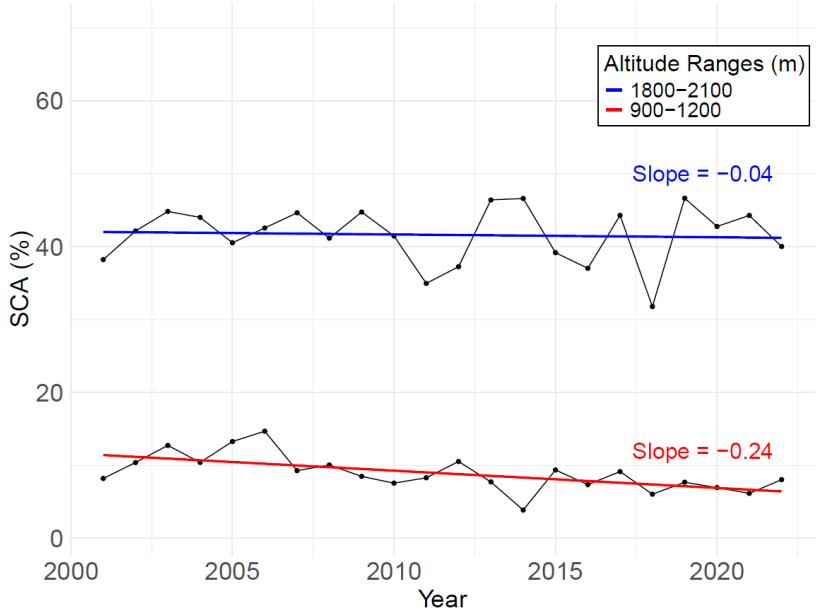

Figure 5.5: SCA for altitude ranges of 900-1200 m (in red) and 1800-2100 m (in blue) in the Danube catchment region

The explanation behind these trends is related to temperature and the altitude of the freezing point. As is well known, the planet's average temperature is rising. This results in increased melting of snow at mid-elevations, but at the same time, there is an increase in winter precipitation. Therefore, regions above the freezing point are characterized by a less negative trend in SCA loss, as these areas continue to experience, if not more, intense snow events.

When observing the overall figures, this trend may not be apparent because averaging over large areas results in a pattern that represents mid-elevation trends. Peaks at higher elevations constitute a small portion of the area, even in regions with presence of mountainous areas. Thus, a large-scale analysis does not reveal what is highlighted through an analysis of specific elevation ranges.

5.2 Austria

5.2.1 Temporal evolution of maximum river discharge

Regarding the second study area, the analysis begins by evaluating runoff data, specifically focusing on peak discharge values recorded at the river measurement stations. Three peak discharge values are assessed annually: the first represents the highest runoff recorded throughout the entire year, while the second and third correspond, respectively, to the seasonal peak discharge during the winter and spring months.

As examples, we selected one station per region to illustrate the temporal evolution of peak discharge, including the maximum yearly values and the winter and spring peaks, based on data availability.

The chosen stations are the number: 201236 for the alpine region, 212670 for the southern alpine region, 201087 for the northern alpine region, 204750 for the northern lowlands and 210211 for the eastern lowlands. In Table 6 are reported the station numbers together with their corresponding characteristics.

Figure 5.6, Figure 5.7 and Figure 5.8 illustrate the alpine region, southern alpine region and eastern lowlands, which exhibit the most interesting behaviours. The remaining two regions are reported in the appendix A.1.

Station number	River name	Station location	Catchment area (km^2)	Outlet elevation (m)
201236	Trisanna	See	385.4	1017.0
212670	Gail	Rattendorf	594.9	595.3
201087	Lech	Lechaschau	1012.2	836.1
204750	Antiesen	Haging	164.9	378.7
210211	Lafnitz	Dobersdorf	925.1	234.0

Table 6: Characteristic of five selected stations: number, river name, location, catchment area and outlet elevation

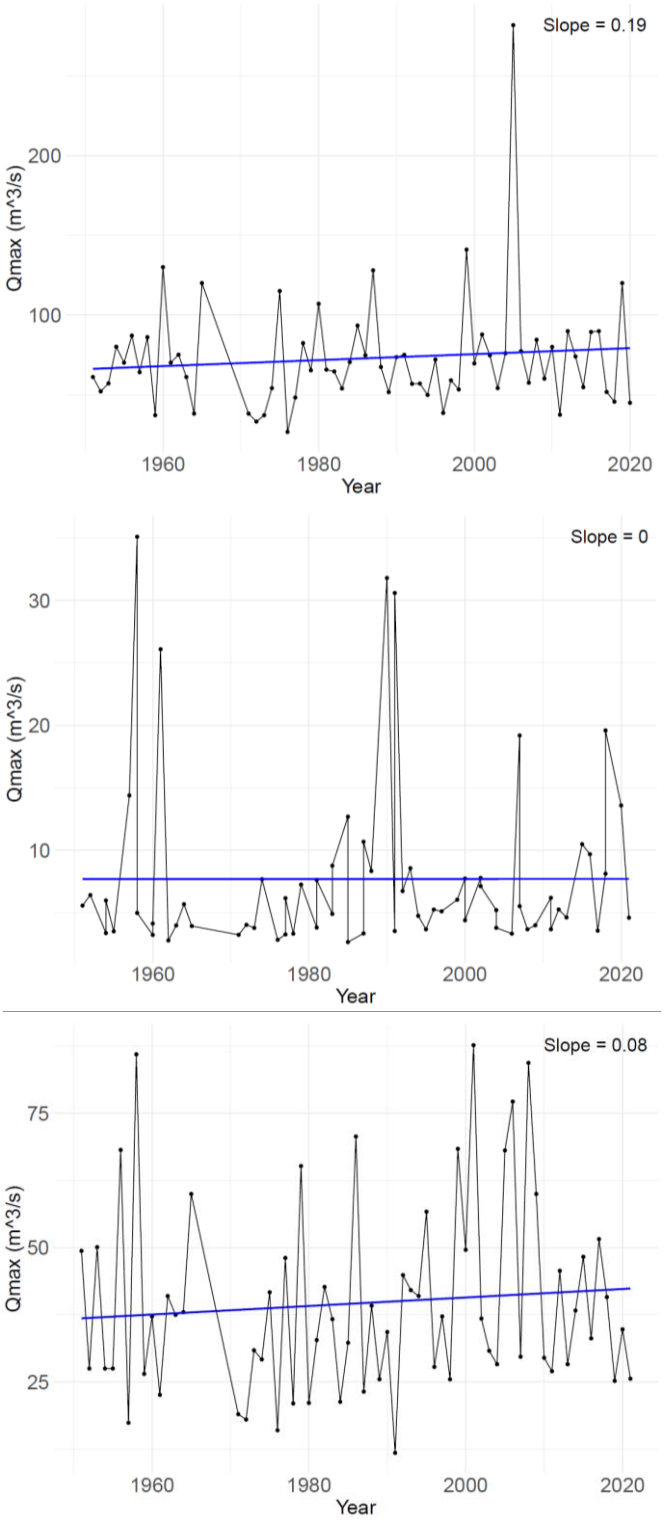

Figure 5.6: Annual and seasonal (winter and spring) maxima peak discharges at alpine region's station nº 201236. River: Trisanna. Location: See.

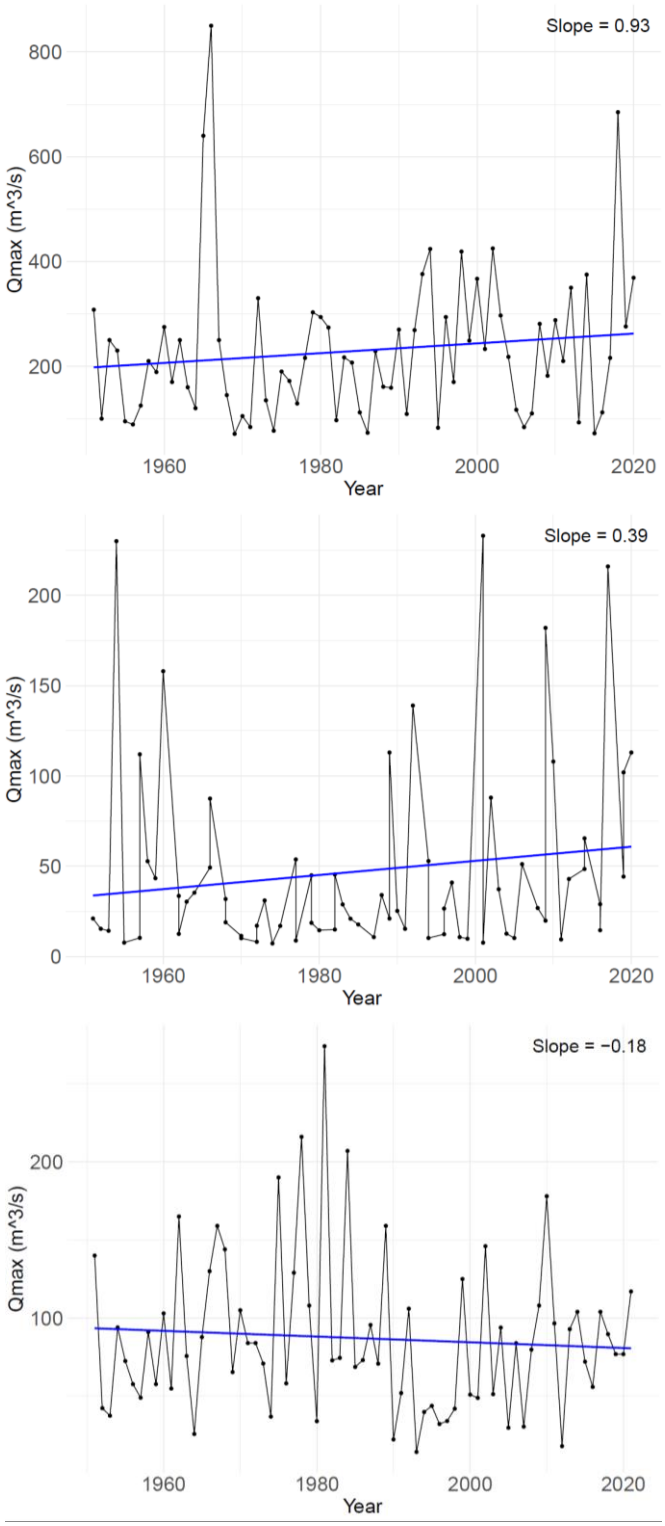

Figure 5.7: Annual and seasonal (winter and spring) maxima peak discharges at southern alpine region's station n° 212670. River: Gail. Location: Rattendorf

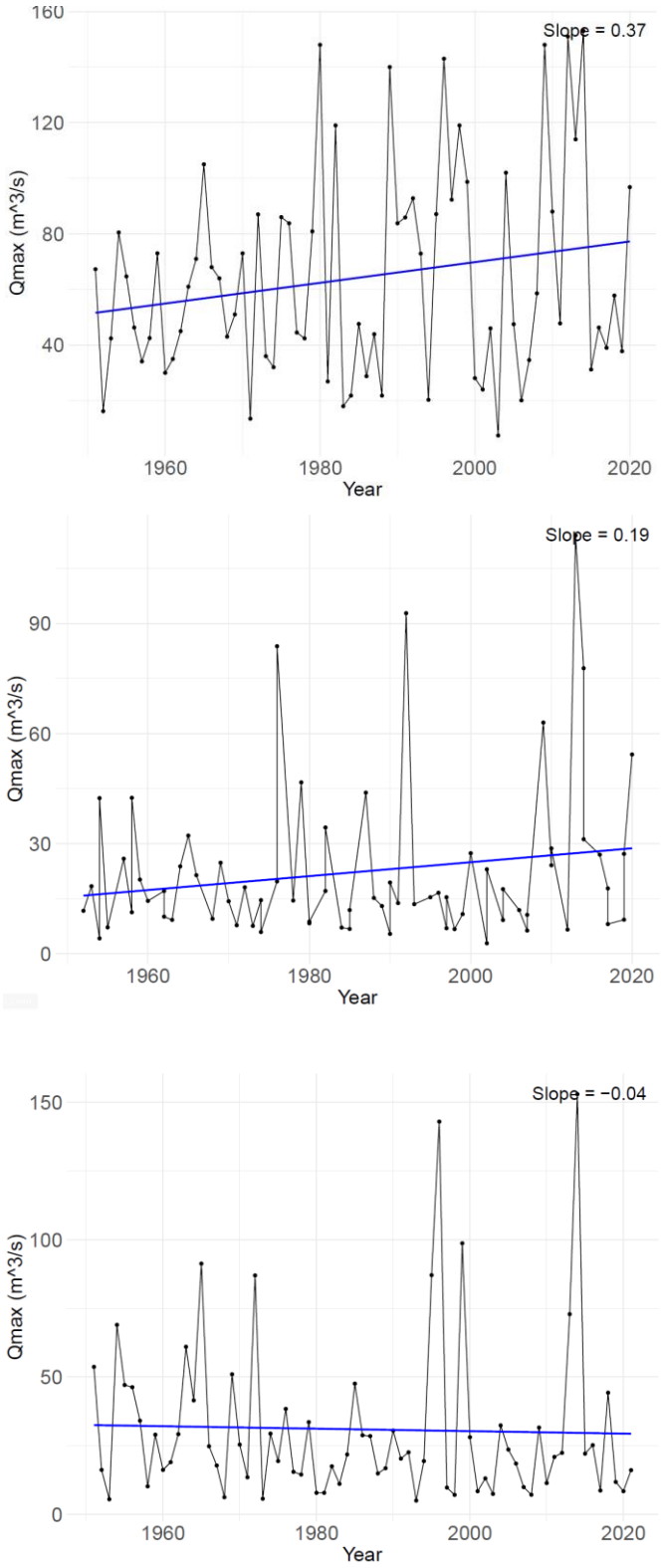

Figure 5.8: Annual and seasonal (winter and spring) maxima peak discharges at southern alpine region's station n° 210211. River: Lafnitz. Location: Dobersdorf

For all five stations, it is observable an increasing trend in annual peak values. It is notable, however, that the peak trends in the winter and spring seasons can differ and, in some cases, be opposite to the annual series.
Specifically, for station number 212670 in the southern alpine region and station number 210211 in the eastern lowlands, the trends have opposite sign in different seasons: positive and aligned with the annual series in winter, but negative and thus contrary to the annual values for spring floods.
Table 7 provides the average trend values for the linear trends of the annual series over the three reference periods (annual, winter and spring) for the five defined regions and for Austria as a whole.

Regions	Qmax slope (m^3/s/year)	Winter Qmax slope (m^3/s/year)	Spring Qmax slope (m^3/s/year)
Alpine	0.12	0.25	0.07
Southern alpine	0.13	0.19	- 0.12
Northern alpine	0.24	0.32	- 0.02
Northern lowlands	0.14	0.08	0.01
Eastern lowlands	0.13	0.09	0.02
Total	0.15	0.17	- 0.03

Table 7: Average slope values of the linear trends of maximum discharge in a year, during winter and spring, of the stations contained in the five regions of interest and over the state of Austria

The linear trend of annual peak values over time shows a roughly comparable growth pattern across the regions of Austria. However, significant differences emerge between regions in the trends of seasonal peaks. Winter peaks are either more or less increasing in time compared to the growth rates of annual peaks, depending on the region, while spring peaks are either slightly increasing or decreasing, with an overall negative linear trend across Austria.

Trying to give an explanation of these observed behaviours, linking them with the region's characteristics, one can notice, for example, the difference between the alpine and northern alpine regions.
The northern alpine region experiences the highest rainfall in Austria, largely due to the orographic effects of the Alps. In this area, significant rainfall leads to frequent

summer floods, primarily driven by frontal weather patterns with minimal influence from snowmelt. The values in the table align with this description, showing that a progressive increase in discharge during peak annual and winter events is accompanied by a decrease in spring peak discharge due to minimal influence from snowmelt.
In contrast, the increasing trend in spring flood events in the alpine region is due to the fact that the alpine region is notably influenced by snow and glacier melt. Although most floods occur during the summer, early summer floods are often preceded by snowmelt.

5.2.2 Temporal evolution of Snow-Covered Area

Just like for study area number one, the temporal trend of SCA is evaluated also for all the Austrian catchments under examination. The mean was then calculated to obtain an annual value per each catchment, which was subsequently averaged for the five regions of interest to assess how snow cover behaves depending on the presented characteristics. Finally, a national average was obtained to provide an overview. The results are shown in Figure 5.9.

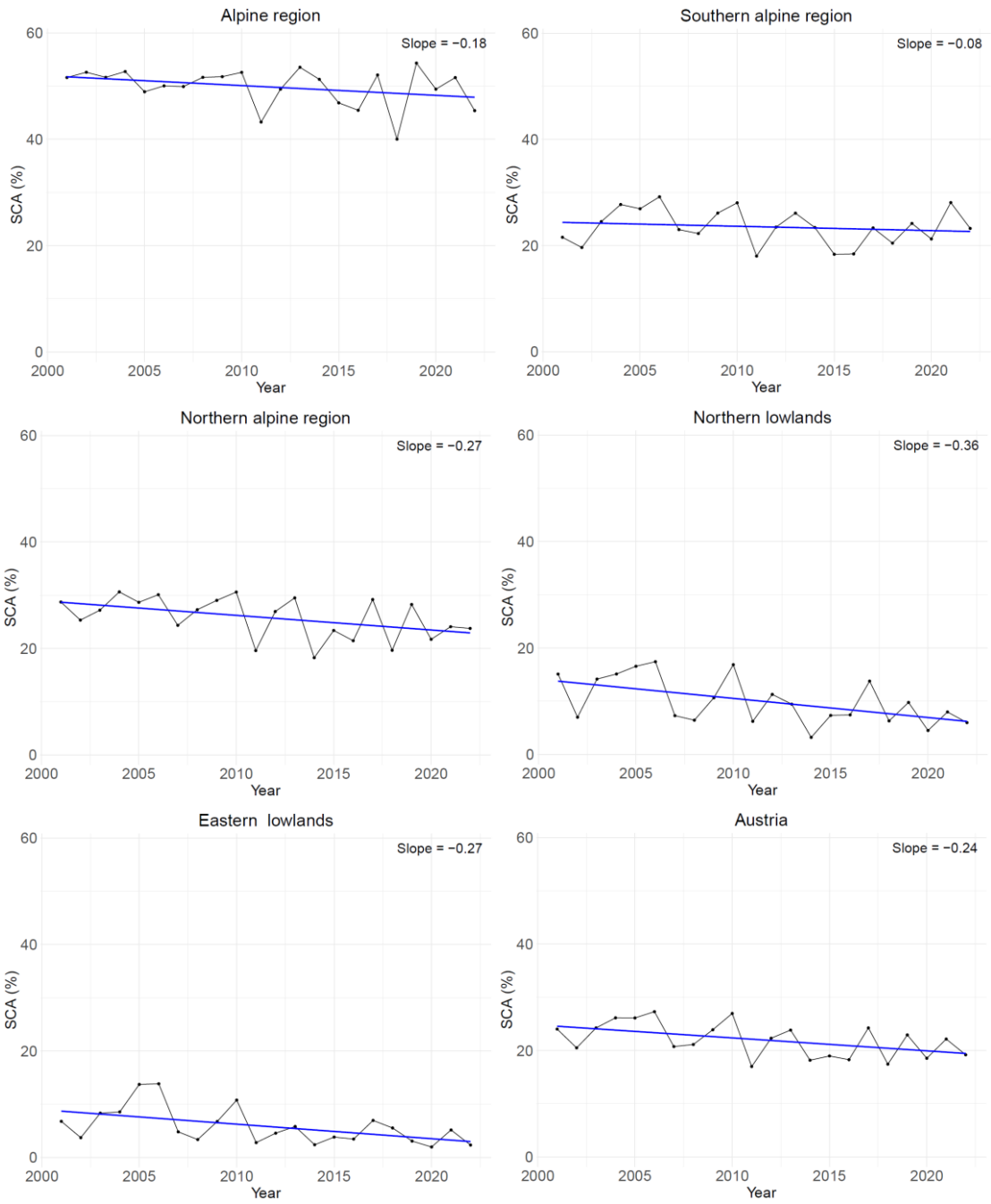

Figure 5.9: Evolution of Snow-Covered Area in the time period 2001-2022, averaged 1 value per year, evaluated for the five different regions of Austria and the entire country

Table 8 summarizes the results presented in Figure 5.9 for the five regions of interest, including a column for the p-value calculated using the Mann-Kendall test to assess the linear trend of the average values over time for these regions.

Regions	Slope of SCA (%/year)	Mann-Kendall test, p-value
Alpine	-0.18	0.19
Southern alpine	-0.08	0.57
Northern alpine	-0.27	0.07
Northern lowlands	-0.36	0.04
Eastern lowlands	-0.27	0.01
Total	-0.24	0.06

Table 8: Slope and p-value of the interpolating linear trend of the SCA values in the period 2001-2022, evaluated for the five different hydrological Austrian regions and the entire country

Regarding the alpine region, the slope for SCA shows a negative trend, indicating a reduction in snow cover over time. However, the Mann-Kendall p-value is not statistically significant (> 0.05), suggesting that even though there is a downward trend, there is insufficient evidence to confirm it is meaningful.

The southern alpine region shows a slight decrease in snow-covered area over time, with a slope near zero. The high p-value indicates that the decrease is not statistically significant. Therefore, the small change in SCA is likely due to natural variability rather than a real trend.

In the northern alpine region, the slope indicates a strong decreasing trend in SCA over time, with the Mann-Kendall p-value (0.07) slightly exceeding the 0.05 threshold.

The northern lowlands region shows the steepest decline in SCA (-0.36), and the Mann-Kendall test confirms that the trend is statistically significant. This indicates that the reduction in snow cover is real and not due to random chance.

A significant decrease in snow-covered area is observed as well in the eastern lowlands. The Mann-Kendall p-value is below 0.05, confirming that the trend is clearly significant.

Nationally, the reduction in SCA is quite significant, with the Mann-Kendall test indicating a p-value of 0.06, which is slightly above the significance threshold.

5.2.3 Antecedent snow cover conditions for peak discharge

In this chapter, it is represented the snow cover trends leading up to a river flood event. The average snow cover is calculated for the years in question during the week preceding the event, the second-to-last week and the third-to-last week before a flood event, both for the winter and spring periods.

To estimate snowmelt, the difference between the average snow cover from the second-to-last week and the week before the flood event is calculated, as well as the difference between the third-to-last week and the last week before the flood event.

The linear trend over time for these temporal patterns is determined, and the p-values assessed using the Mann-Kendall method to verify their statistical significance.

Here we present the results for the snow cover one week before the flood event (SCA 1 week before Qmax) and the change in snow cover between the second-to-last and the last week (Delta SCA 2-1 weeks before Qmax), along with their statistical values for the winter (Figure 5.10, Table 9, Figure 5.11, Table 10) and spring months (Figure 5.12, Table 11, Figure 5.13, Table 12), averaged for the five different regions of Austria and over the entire country. Due to similarity in the results, we include in the appendix A.2 the average snow cover two and three weeks before the flood event, as well as the difference between the third-to-last and the last week before the event, again for both winter and spring periods.

– *SCA 1 week before Qmax over time (winter):*

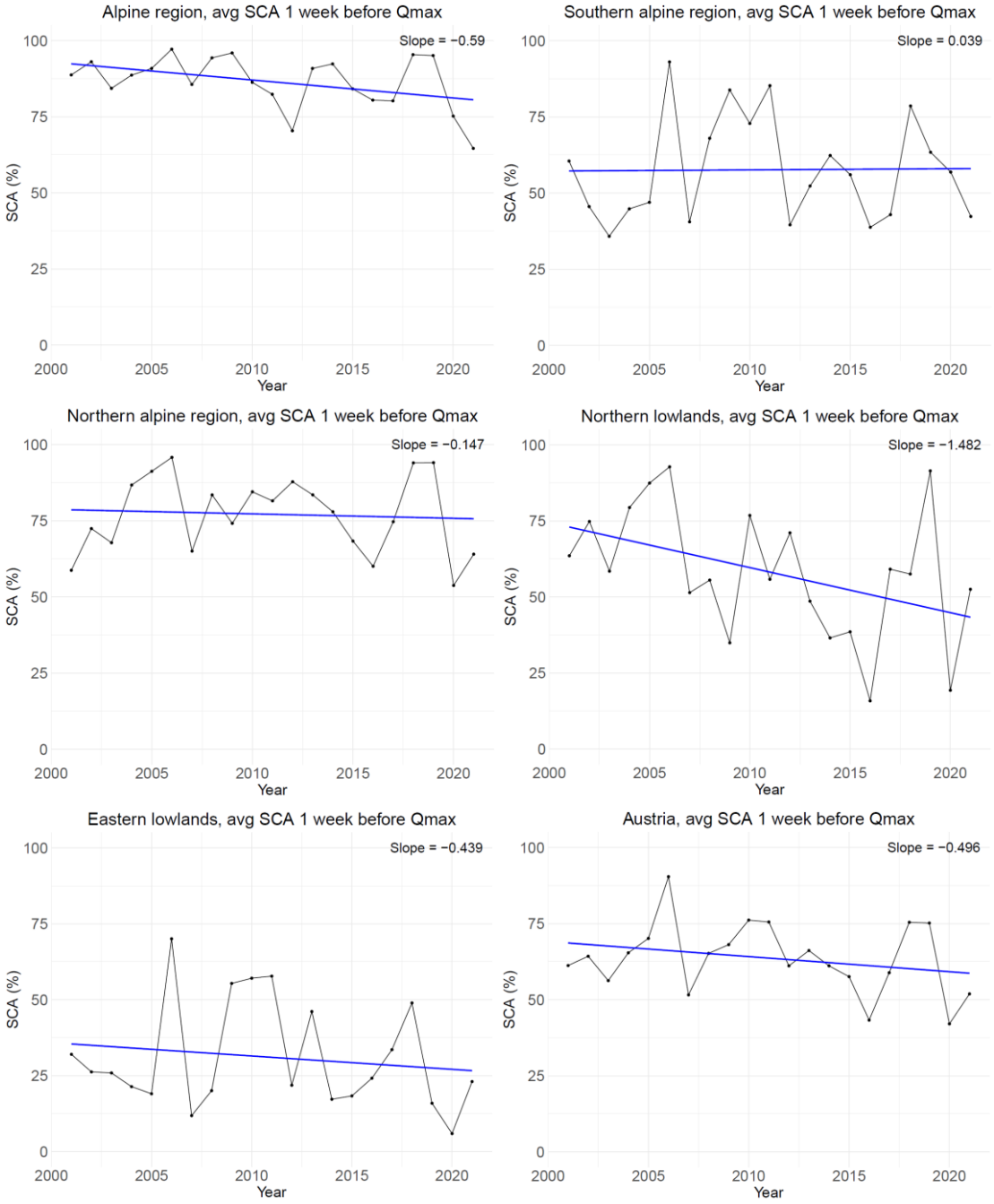

Figure 5.10: Snow-Covered Area during the seven days before the event of maximum in discharge registered in the winter season, from 2001 to 2022, averaged for the five different regions of Austria and over the entire country

Regions	Slope of SCA 1 week (%/year)	Mann-Kendall test, p-value
Alpine	-0.59	0.11
Southern alpine	0.04	0.98
Northern alpine	-0.15	0.88
Northern lowlands	-1.48	0.08
Eastern lowlands	-0.44	0.29
Total	-0.50	0.32

Table 9: Slope and p-value of the interpolating linear trend of SCA 1 week before a peak in discharge in the winter seasons, 2001-2022, averaged for the five different regions of Austria and over the entire country

Northern lowlands region shows the strongest evidence of a significant decrease in snow cover before winter floods, with Mann-Kendall p-value close to the significance threshold.
The alpine region also shows a notable decline in snow cover, though the trend's significance is above the threshold.
In other regions, such as the southern alpine and northern alpine, trends are minimal or non-existent, with no significant changes in snow cover over time.
Across Austria, while there is an overall decline in snow cover before winter flood events, this decrease is not statistically significant.

– *Delta SCA 2-1 weeks before Qmax over time (winter):*

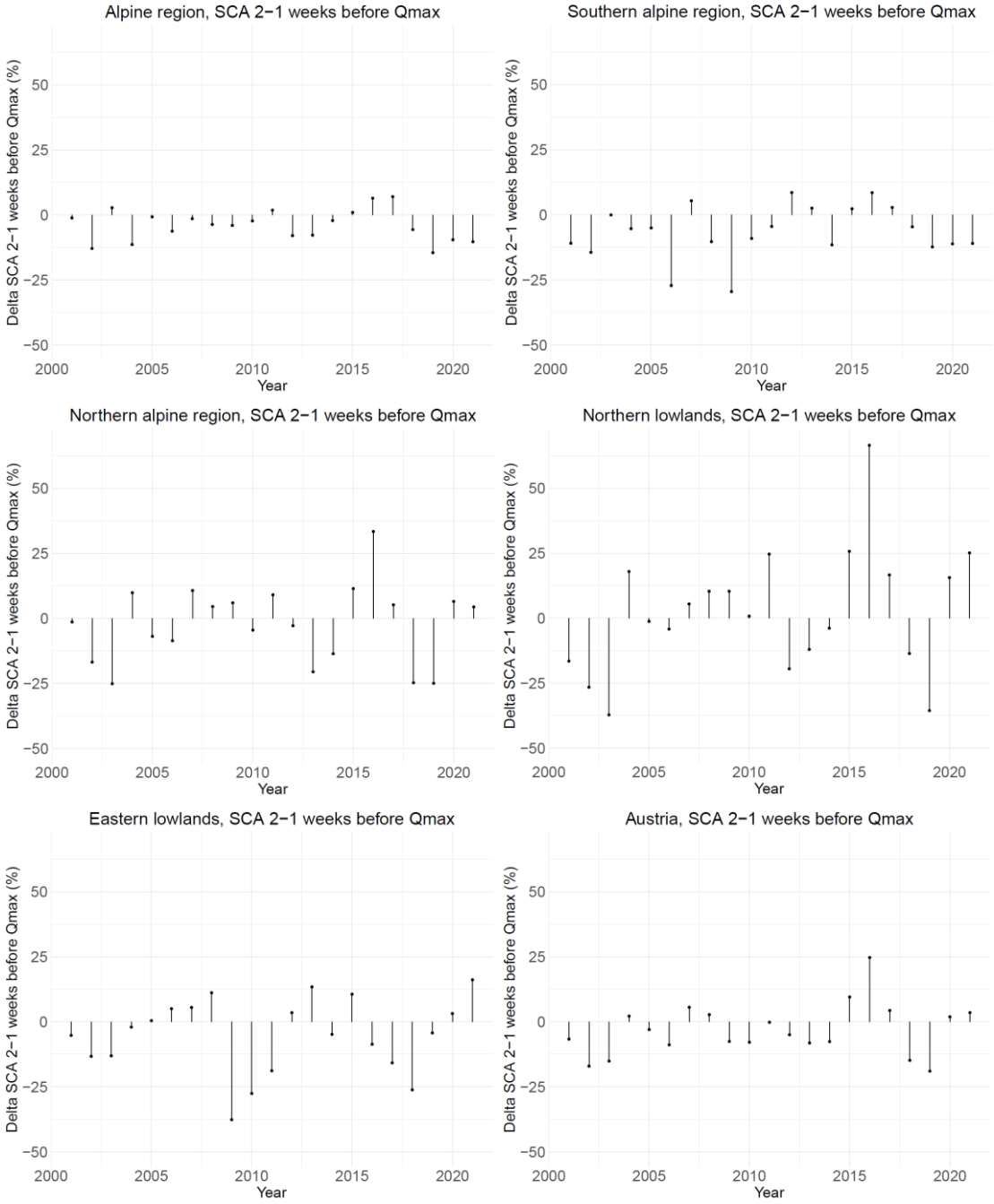

Figure 5.11: Difference between the values of Snow-Covered Area the second and the first week before the event of maximum in discharge is registered in the winter season, from 2001 to 2022, averaged for the five different regions of Austria and over the entire country

Regions	Slope of Delta SCA 2-1 weeks (%/year)	Mann-Kendall test, p-value
Alpine	-0.06	0.69
Southern alpine	0.29	0.61
Northern alpine	0.27	0.74
Northern lowlands	1.33	0.11
Eastern lowlands	0.26	0.38
Total	0.42	0.35

Table 10: Slope and p-value of the interpolating linear trend of Delta SCA 2-1 week before a peak in discharge in the winter seasons, 2001-2022, averaged for the five different regions of Austria and over the entire country

The information we can derive from the graphs in Figure 5.11 pertains to the difference between the average snow cover value in the basins during the penultimate and the last week before the peak flow event.
Values on the y-axis less than zero indicate that the average snow-cover area value two weeks before the peak is lower than the average SCA in the week preceding the peak discharge (Qmax). This suggests the occurrence of precipitation events, either rain or snow, which is characteristic of winter seasons.
Conversely, positive values indicate that the average SCA two weeks before the seasonal peak flow is higher than the average SCA in the week before the peak discharge. This suggests a decrease in snow cover leading up to the peak, likely due to snowmelt, a phenomenon typical of spring seasons.
The slope values in Table 10 indicates whether this snowing/melting behaviour has increased or decreased over the past two decade.

– *SCA 1 week before Qmax over time (spring):*

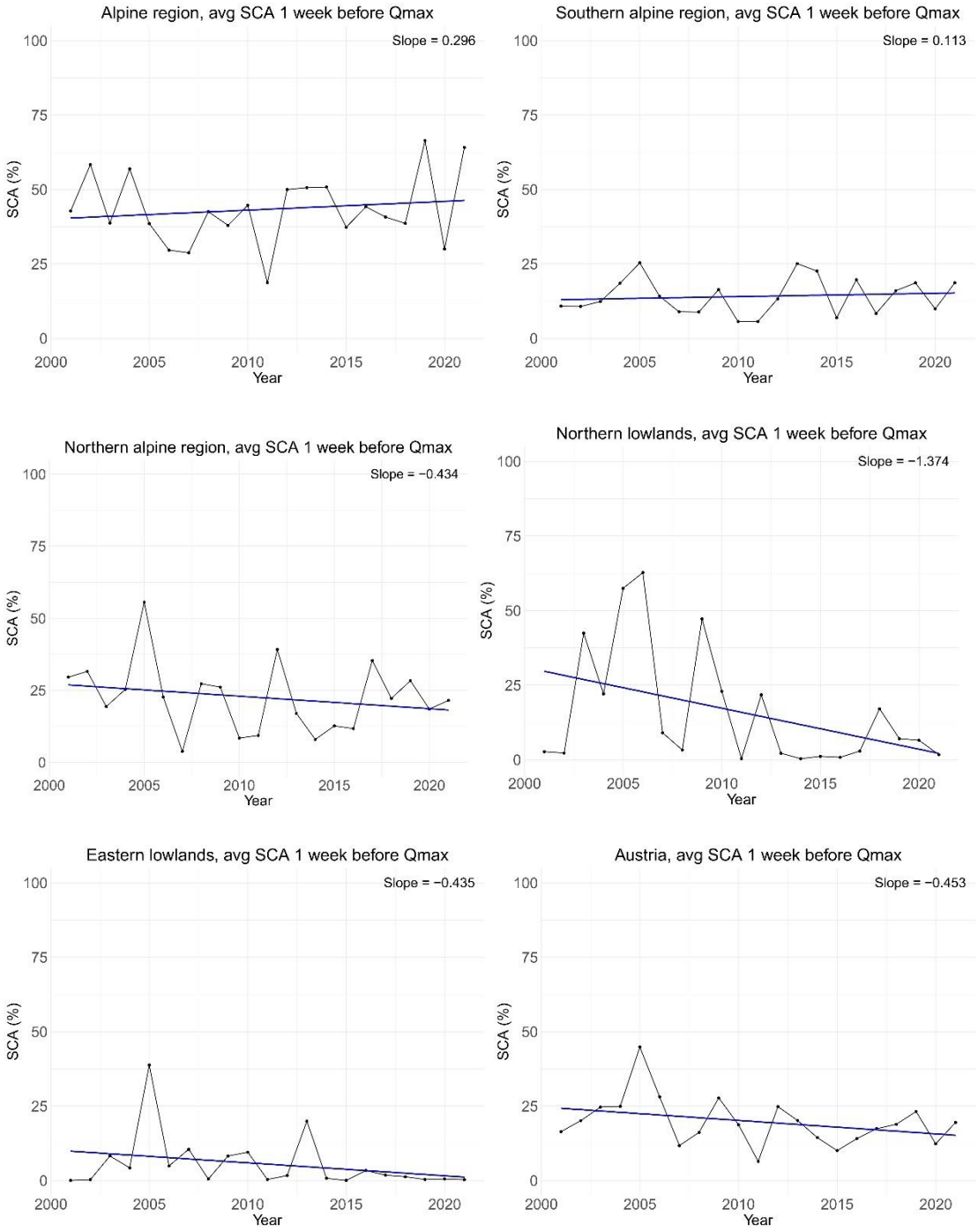

Figure 5.12: Snow-Covered Area during the seven days before the event of maximum in discharge registered in the spring season, from 2001 to 2022, averaged for the five different regions of Austria and over the entire country

Regions	Slope of SCA 1 week (%/year)	Mann-Kendall test, p-value
Alpine	0.30	0.74
Southern alpine	0.11	0.69
Northern alpine	-0.43	0.41
Northern lowlands	-1.37	0.11
Eastern lowlands	-0.44	0.22
Total	-0.45	0.24

Table 11: Slope and p-value of the interpolating linear trend of SCA 1 week before a peak in discharge in the spring seasons, 2001-2022, averaged for the five different regions of Austria

Comparing Table 11 with Table 9, which presents the winter season, a significant difference in behaviour can be observed between the alpine and northern alpine regions. In the alpine region, there is an increase in snow cover during the week preceding a spring flood, contrasting with the winter period, which shows a descending linear trend. In the northern alpine region, however, the trend is more negative in spring compared to winter, likely due to stronger snowmelt processes in spring.

For the other three regions, the behaviour is more or less consistent with that observed in winter. While the slope values indicate variations in snow cover before flood events, the Mann-Kendall test reveals that, overall, the trends are not statistically significant across the five regions and Austria.

– *Delta SCA 2-1 weeks before Qmax over time (spring):*

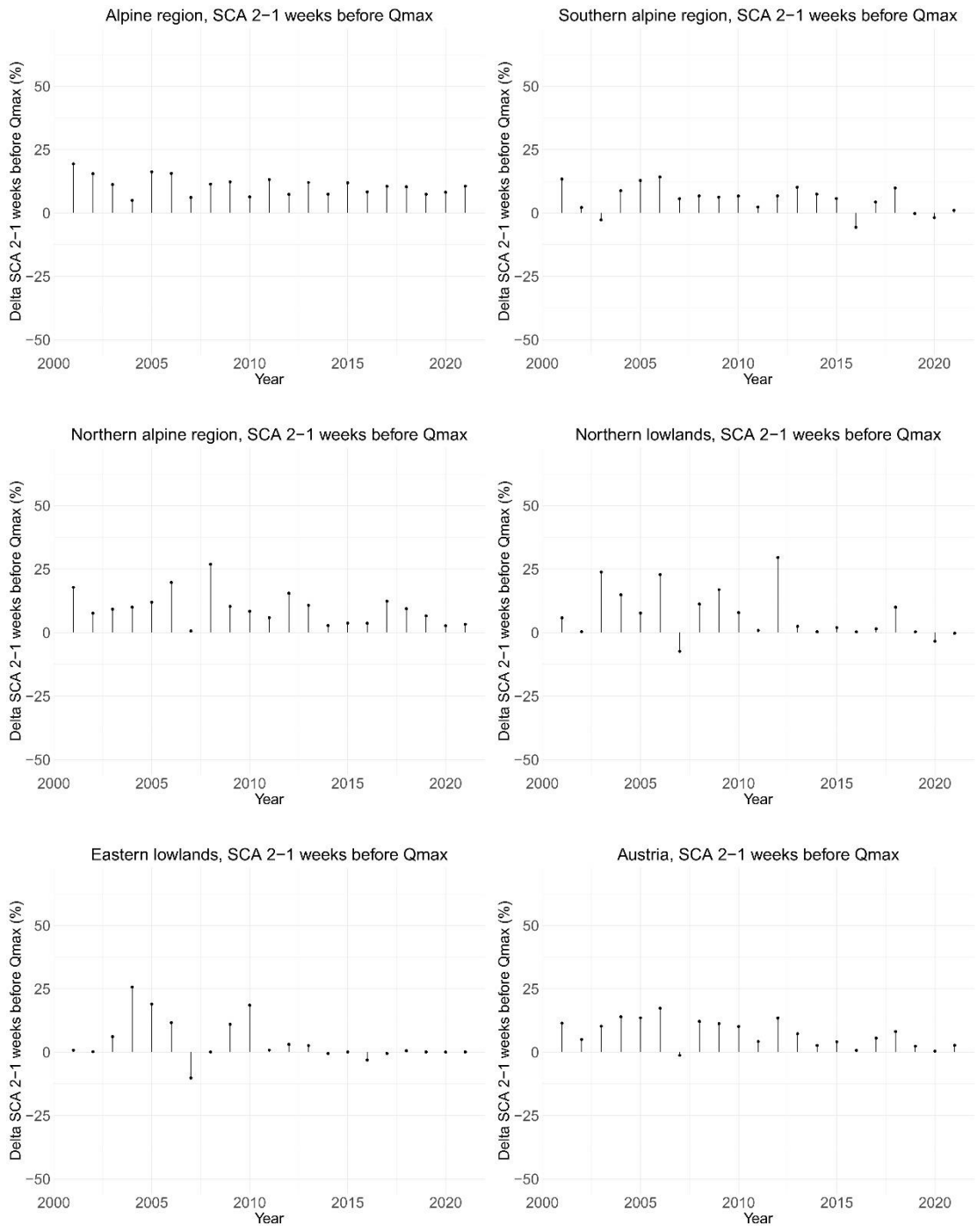

Figure 5.13: Difference between the values of Snow-Covered Area the second and the first week before the event of maximum in discharge is registered in the spring season, from 2001 to 2022, averaged for the five different regions of Austria and over the entire country

Regions	Slope of Delta SCA 2-1 weeks (%/year)	Mann-Kendall test, p-value
Alpine	-0.27	0.12
Southern alpine	-0.35	0.08
Northern alpine	-0.45	0.06
Northern lowlands	-0.61	0.02
Eastern lowlands	-0.54	0.04
Total	-0.49	0.01

Table 12: Slope and p-value of the interpolating linear trend of Delta SCA 2-1 week before a peak in discharge in the spring seasons, 2001-2022, averaged for the five different regions of Austria and over the entire country

Referring to what was highlighted in the comments of the graphs shown above in Figure 5.11 regarding the winter season, it can be observed that most of the delta values before a peak event are positive. This underscores the contribution of snowmelt prior to a flood event. This pattern is particularly noticeable in the alpine regions.

The negative value indicated by the slope in Table 12 may be attributed to the general decrease in snow cover, as observed in Figure 5.9, which varies in different ways by region.

5.2.4 Qmax vs SCA: Scatter Plot and Correlation

We investigated whether there is a correlation between the height of the winter/spring flood peaks and snow cover in the week prior, as well as a correlation between the height of the winter/spring flood peaks and snowmelt between the second-to-last and last week before the flood event.

The graphical result is shown as example only for the first basin of the Austrian database: number 200014, station located in Bangs, evaluating the Rhein River, catchment area of 4647.9 km^2 and outlet elevation of 420 m.

Figure 5.14 displays the Pearson's correlation coefficient and its p-value for both the winter and spring cases.

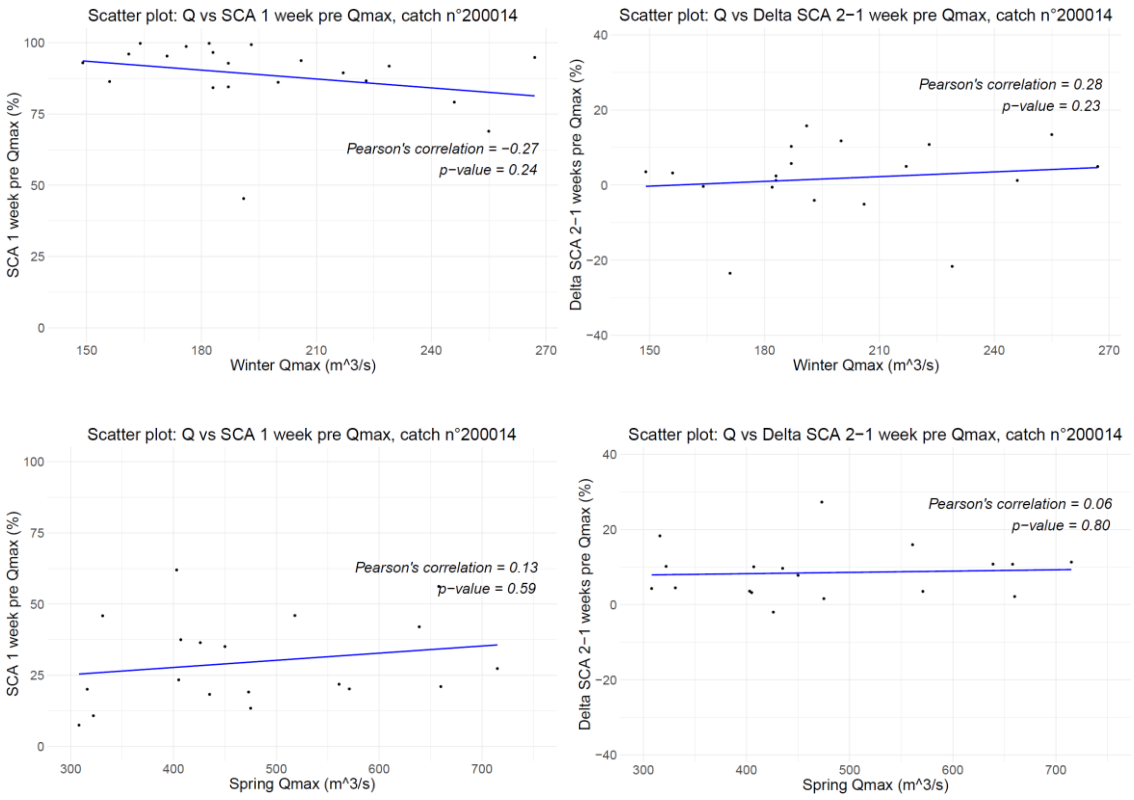

Figure 5.14: Winter and spring Person's correlation coefficients and p-values between Qmax and average SCA 1 week before Qmax, and between Qmax and DeltaSCA 2-1 week before Qmax, for the catchment n° 200014

5.2.5 Boxplots of regional correlations

Once all the correlation values between peak discharge and snow cover in the week preceding the flood event, as well as between peak discharge and the change in snow cover in the two weeks before the flood event, have been obtained for every station, they were grouped by their respective regions.

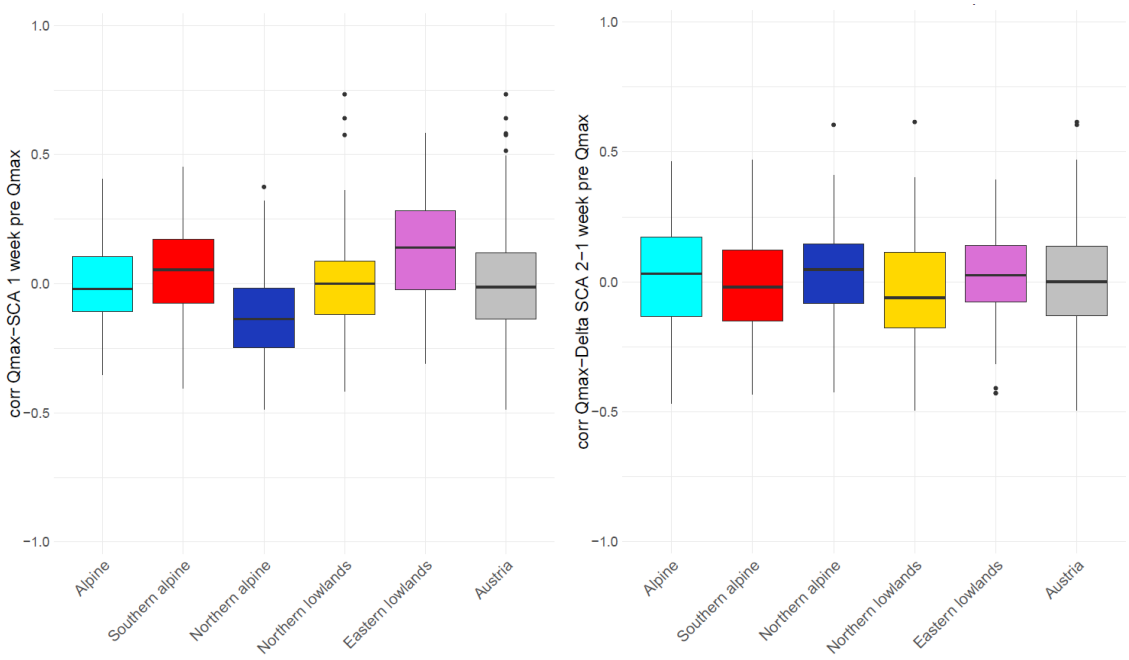

Figure 5.15: Correlation analysis of winter peak discharge - snow cover in the week before peak and of winter peak discharge - difference in snow cover between two weeks before peak

Figure 5.15 shows that the correlation values for winter peak discharge with snow cover in the week before the peak are generally low and not very significant. This suggests that recent snow cover does not have a strong relationship with winter peak discharge in most regions.

Eastern lowlands show a slightly positive correlation (0.1346), indicating a weak but positive relationship between snow cover and peak discharge. This might be linked to the region's exposure to frontal systems that can intensify with snow cover.

The negative correlation of -0.1266 in the northern alpine region suggests that, in this region, as snow cover increases, winter peak discharge tends to slightly decrease, or in contrast, as snow cover decreases, peak discharge tends to increase.

Possible explanations for this behaviour of negative correlation could be attributed to different physical factors. Considering rain-on-snow events, rain falling on snow

can cause snow to melt rapidly, contributing to increased runoff and higher peak discharge, or alternatively it may absorb some of the rainfall if snow cover is higher, which reflects in a reduction of immediate runoff and delaying peak discharge.
Another possible reason could be that in winter a considerable amount of the snow might not melt immediately but instead accumulate and contribute to runoff later in the season, particularly during spring. As a result, when snow cover is high, peak discharge might be delayed, leading to lower discharge in the immediate term.
Lastly, one could say that the snowpack can act as insulator and reduce the amount of snowmelt that contributes to discharge during cold periods that could translate in lower peak runoff when snow cover is more abundant.

Looking at the right panel of Figure 5.15, also in this case the correlations are quite low, suggesting minimal impact of changes in snow cover over two weeks on winter peak discharge.
The values being close to zero across most regions indicate that variations in snow cover over the two weeks do not strongly influence winter peak discharge.

Figure 5.16 illustrates the same correlation parameter but for the spring season.

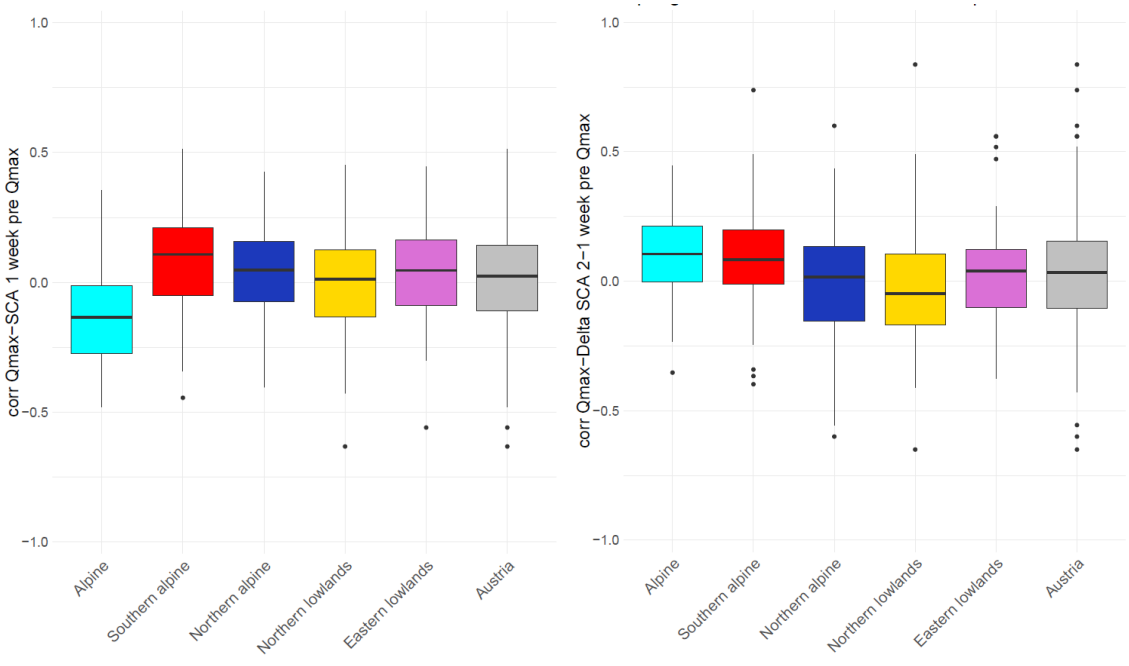

Figure 5.16: Correlation analysis of spring peak discharge - snow cover in the week before peak and of spring peak discharge - difference in snow cover between two weeks before peak

Observing the left panel, it can be evaluated that the correlation values are again generally low. The negative correlation in the alpine region (-0.1215) indicates a weak negative relationship between snow cover and spring peak discharge. This suggests that higher snow cover might be associated with lower peak discharge or, the other way around, that an increase in peak discharge could be linked to lower snow cover in the week before the event. This could happen due to early snowmelt or other factors such as rain-on-snow events, where increased runoff from rain accelerates snowmelt, leading to higher discharge while reducing snow cover.
The southern alpine region shows a small positive correlation (0.0888) between snow cover and peak discharge. Mediterranean weather systems, which frequently bring moist air and precipitation, play a key role in in this region. They can increase soil moisture before a flood event, making the region more prone to runoff when snowmelt occurs or during additional rainfall, or they can interact with snowmelt processes, where rain may combine with snowmelt, leading to increased runoff.

Examining the right panel of Figure 5.16, we can say that the correlations are low but positive in most regions, suggesting a slight relationship between the change in snow cover and spring peak discharge. This is consistent with the observed effect of snowmelt on peak discharge in regions with significant snow cover.
The northern alpine region shows a very low correlation, which aligns with the observation that snowmelt has less impact on flooding in this area due to high rainfall and less snow influence.

5.2.6 *Behaviour of correlation values with Area and Elevation*

To better understand the behaviour of runoff floods and snow cover evolution in the five chosen subject areas, we broaden this study by looking at each value of correlations of every single catchment in relation to its area and elevation.
Here is reported the most interesting graph showing the spring correlation between peak discharge and snow cover during the week pre peak event in relation to the elevation of the catchment outlet, that provide additional insights beyond what was revealed in the previous chapter through the analysing of the boxplots.
Appendix A.3 contains the other graphs showing the correlations between peak discharge and snow cover in the week before the event, as well as the difference in snow cover between the last two weeks before the event, in relation with area and elevation for the winter or spring period.
The graphs are presented with a logarithmic x-axis to better represent the results, as most catchments have relatively low values of area and elevation compared to the total range of catchments. The coloured interpolating lines in these graphs have just the purpose to try to better visualize the average behaviour of the points representing the regions.
Filled circles represent values of correlations with associated p-value > 0.05, while empty circles are the one related to a significant trend.
Figure 5.17 shows the correlation between peak discharge and snow cover in the week prior to the peak.

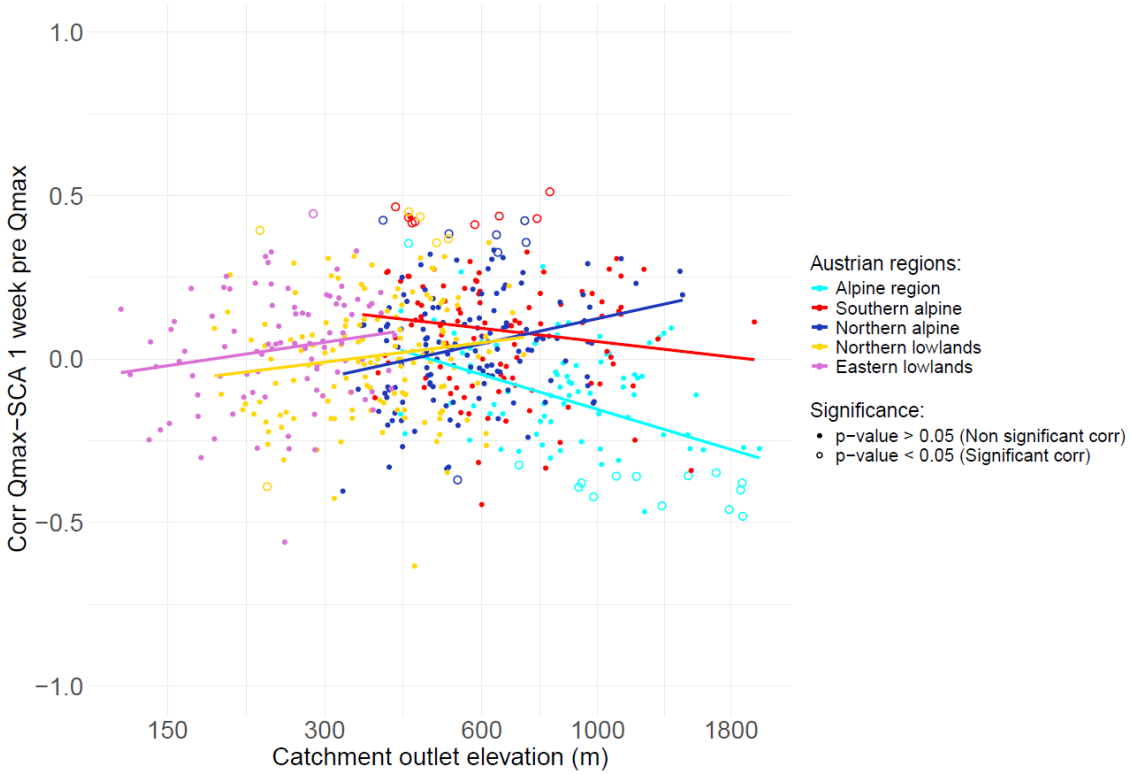

Figure 5.17: Spring correlation between peak in discharge and average SCA one week before a maximum in discharge, in relation to the elevation of the catchments in the five Austrian regions

In the alpine region, as elevation increases, the negative correlation between spring peak discharge and snow cover becomes stronger. This suggests that at lower elevations, there might be a weak association between snow cover and runoff, meaning that increases in snow cover slightly correspond with increases in runoff or vice versa. However, at higher elevations, the relationship becomes more negative, indicating that as snow cover decreases, runoff tends to increase, or as snow cover increases, runoff tends to decrease.

These behaviours could both be possible. In the first case, snowmelt in spring is more pronounced at higher elevations due to greater snow accumulation and to the contribution of glacier melt, which affects river discharge. The second phenomenon could be explained by precipitation events occurring in the week prior to a flood event, where at higher elevations, precipitation may fall as snow. Consequently, the deposited snow does not immediately affect river discharge, as instead is the case at lower elevations, below the freezing level, where rainfall occurs.

In the southern alpine region, the positive correlation decreases with elevation. At lower elevations, increases in snow cover are associated with increases in runoff, or decreases in snow cover are associated with decreases in runoff. However, as elevation increases, this relationship weakens, approaching zero. This could be due to the influence of Mediterranean storm systems at higher elevations, which might diminish the effects of snow cover on runoff. As a result, snowmelt's impact on runoff becomes less pronounced with increasing elevation.

In the northern alpine region, the correlation trend is positive with increasing elevation. At lower elevations, a negative correlation indicates that as snow cover increases, runoff tends to decrease, or as snow cover decreases, runoff tends to increase. At higher elevations, this trend shifts to a positive correlation, meaning that increases in snow cover are associated with increases in runoff, or decreases in snow cover correspond to decreases in runoff. This shift could be due to the higher rainfall and orographic effects at higher elevations enhancing the role of snowmelt in contributing to runoff.

The northern lowlands show high variability in the correlation, averaging around zero. This suggests that the relationship between snow cover and runoff is inconsistent. In this flat terrain with lower precipitation, snow cover's impact on runoff is minimal, leading to unpredictable correlations.

The eastern lowlands have a generally modest positive correlation. This indicates that increases in snow cover are weakly associated with increases in runoff, or decreases in snow cover correspond to decreases in runoff. Despite the generally low snowfall and minimal impact of snow cover, there is still a weak positive relationship, suggesting that snow cover has a small but discernible effect on runoff in this region.

In summary, it can be said that variations in correlation trends with elevation reflect how snow cover's impact on runoff differs by region, influenced by climatic factors, precipitation patterns, and elevation-specific characteristics.

6 Discussions and conclusions

This thesis aimed to investigate the spatiotemporal patterns of snow cover and its influence on flood events, specifically snowmelt-induced floods, by using MODIS satellite data from the Terra and Aqua sensors. The analysis was conducted across two primary regions: the large-scale Danube River basin, encompassing a diverse range of sub-catchments, and Austria, where a more focused investigation was carried out. By utilizing snow cover and river discharge data from 2001 to 2022, the study aimed to uncover both broad trends and regional variations in snow cover dynamics and their subsequent effects on flood generation.

The first part of the study focused on the Danube River basin, analysing snow cover trends across 104 sub-catchments. MODIS satellite data were processed to extract daily snow cover information, from which annual mean snow-covered areas (SCA) were calculated for each catchment. The findings revealed a clear overall decreasing trend in snow cover throughout the Danube basin, but the rate of decline varied significantly between sub-catchments. Catchments with significant snow presence, such as Inn and Bistrita, exhibited the most pronounced decreases in snow cover, with steep negative slopes indicating faster snow loss over time. In contrast, catchments with lower snow presence, like Arges and Velika Morava, showed less severe declines.

The temporal evolution of SCA was also evaluated across different elevation bands within the Danube basin, revealing important patterns. Contrary to initial expectations, the mid-elevation ranges between 1800 and 2100 meters showed a more stable snow cover trend compared to lower ranges, such as 900 to 1200 meters, which experienced greater losses. This result suggests that while lower elevations are more susceptible to rising temperatures and rapid snowmelt, higher elevations still retain enough cold conditions to sustain winter snow accumulation, although this trend is also declining. The overall results point to a future where snow

cover will continue to decrease, particularly in mid- to low-elevation areas, impacting the hydrological dynamics of the Danube River basin.

In Austria, a more detailed analysis was conducted, focusing on both snow cover and river discharge data collected from 581 river measurement stations spread across five hydrological regions: alpine, southern alpine, northern alpine, northern lowlands, and eastern lowlands. These regions exhibit significant differences in terms of climate, hydrology, and flood generation mechanisms, making Austria an ideal case for examining the relationship between snow cover and flood events. The temporal evolution of SCA in Austria revealed regionally specific trends, with the southern alpine region exhibiting the smallest decline in snow cover.

River discharge data were analysed to track the evolution of annual, winter, and spring peak flows. Across most regions, an increasing trend in annual peak discharge was observed, driven by both snowmelt and precipitation events. However, the seasonal analysis revealed contrasting trends: while winter peak discharge generally showed an upward trend across all regions, spring peak discharges displayed a more complex pattern. In the southern alpine and eastern lowlands regions, spring discharges exhibited a negative trend, suggesting a diminishing contribution of snowmelt to peak floods, likely due to reduced snow accumulation. Conversely, the alpine region, heavily influenced by glacier melt and snowmelt, showed a slight increase in spring peak discharge, in line with its specific hydrological characteristics.

Correlations between snow cover and peak discharge further underscored the complexity of snowmelt processes in flood generation. In the alpine region, a negative correlation between snow cover and peak discharge was observed during spring, indicating that higher snowmelt tends to coincide with lower snow cover preceding flood events. This suggests that as snowmelt increases, contributing to higher river discharges, the amount of remaining snow cover decreases. In contrast, the northern lowlands and eastern lowlands regions displayed weaker correlations, implying that precipitation, rather than snowmelt, is the dominant driver of floods in these areas.

In conclusion, this study demonstrates the intricate role that snow cover dynamics play in flood generation, with significant regional variations observed across both the Danube River basin and Austria. The use of MODIS satellite data provided valuable insights into long-term trends in snow cover, and the analysis of river discharge data offered a deeper understanding of how these trends are linked to flood risks. Future research could build on these findings by taking an additional

step: integrating stochastic modelling. This tool would enable the assessment of how future climate scenarios might influence snow-driven floods by simulating the mechanisms through which these changes occur. Stochastic modelling offers the advantage of generating numerous simulations, allowing for a broader examination of cause-and-effect relationships. Incorporating these relationships into the model would help generalize the effects of different mechanisms on snowmelt runoff dynamics. For example, rising air temperatures could shorten the snowmelt period, leading to earlier flood events, or elevate the snowline, resulting in different flooding characteristics.

Appendix

A.1 Temporal evolution of maximum river discharge

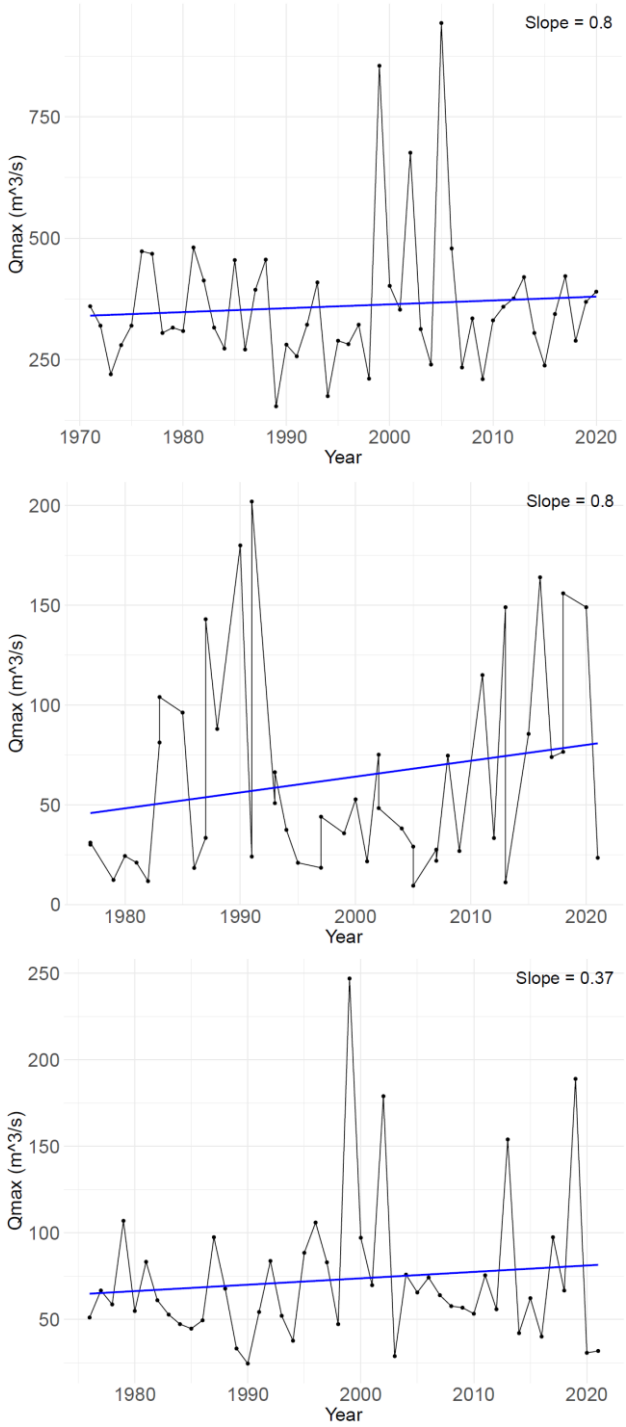

Figure A.1.1: Annual and seasonal (winter and spring) maxima peak discharges at northern alpine region's station n° 201087. River: Lech. Location: Lechaschau.

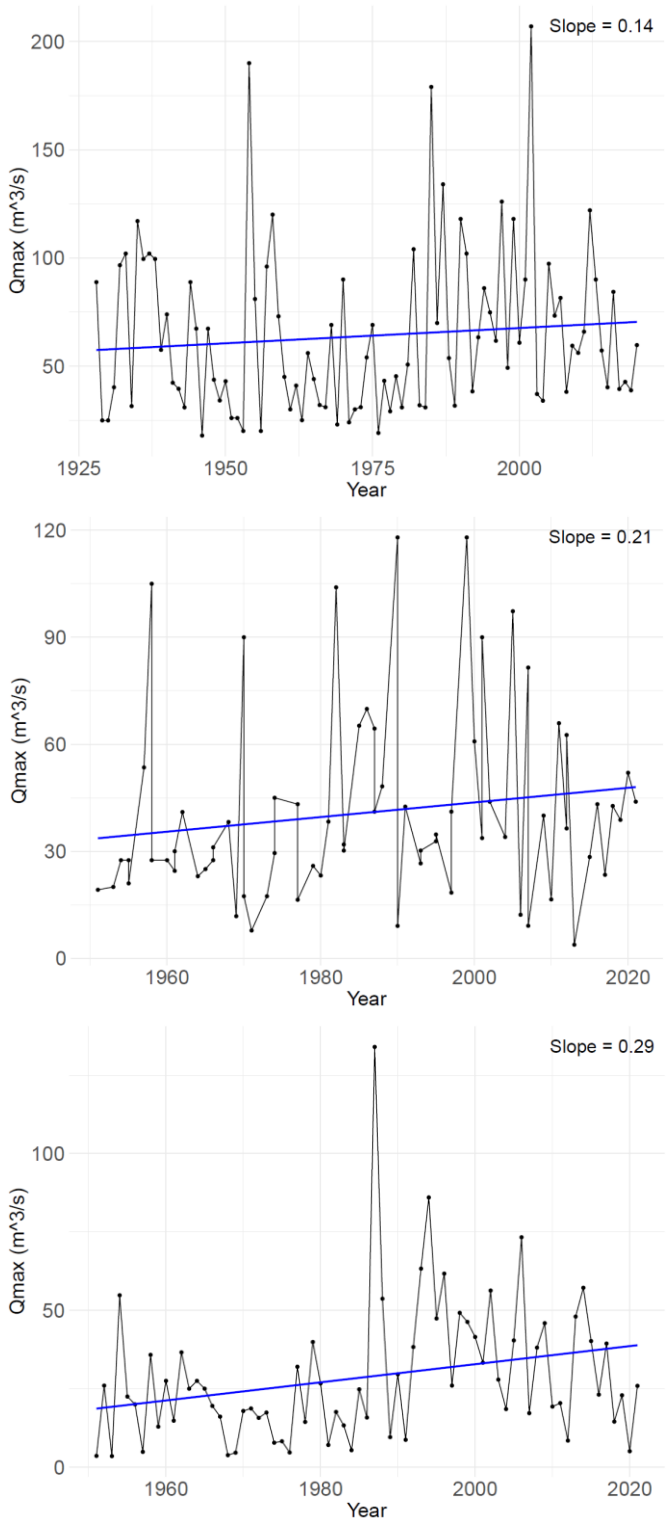

Figure A.1.2: Annual and seasonal (winter and spring) maxima peak discharges at northern alpine region's station n° 204750. River: Antiesen. Location: Haging.

A.2 Antecedent snow cover conditions for peak discharge

– *SCA 2 weeks before Qmax over time (winter):*

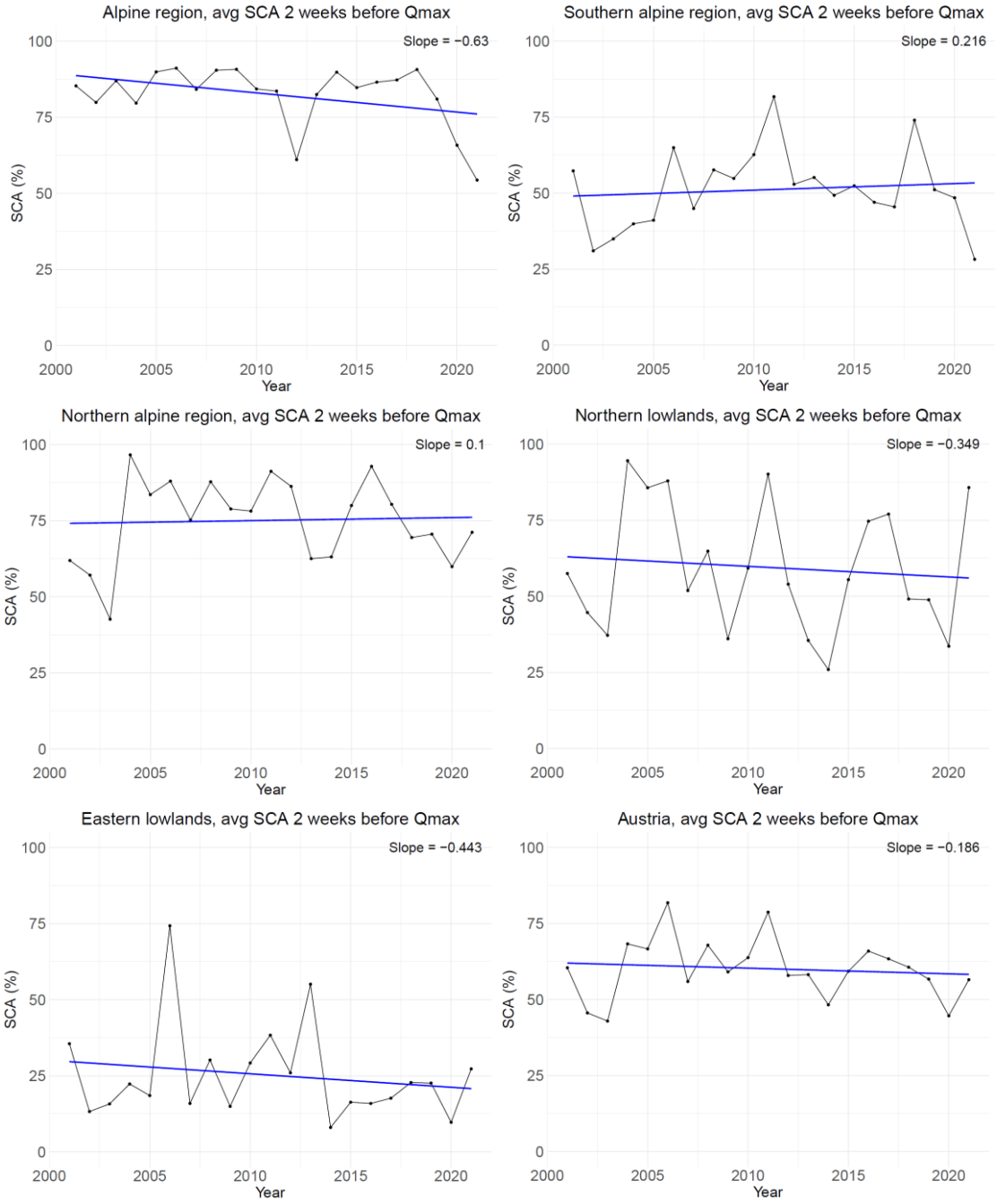

Figure A.2.1: Averaged Snow-Covered Aea from the fourteenth to the seventh day before the event of maximum in discharge registered in the winter season, from 2001 to 2022

Regions	Slope of SCA 2 weeks (%/year)	Mann-Kendall test, p-value
Alpine	-0.63	0.35
Southern alpine	0.22	0.88
Northern alpine	0.10	0.07
Northern lowlands	-0.35	0.45
Eastern lowlands	-0.44	0.83
Total	-0.19	0.35

Table A.1: Slope and p-value of the interpolating linear line of SCA 2 weeks before a peak in discharge in the winter period 2001-2022

– *SCA 3 weeks before Qmax over time (winter):*

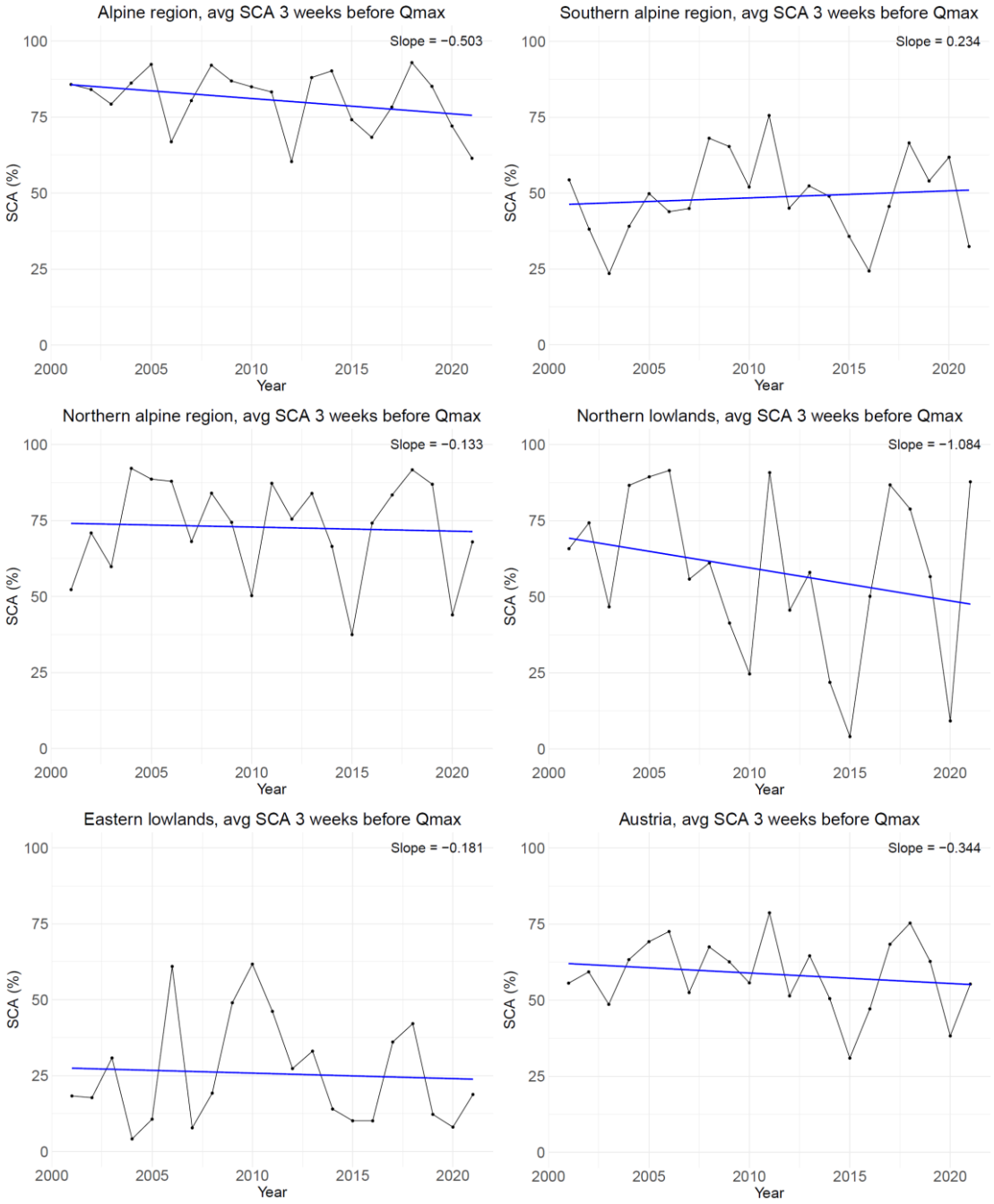

Figure A.2.2: Averaged Snow-Covered Area from the twenty first to the fourteenth day before the event of maximum in discharge registered in the winter season, from 2001 to 2022

Regions	Slope of SCA 3 weeks (%/year)	Mann-Kendall test, p-value
Alpine	-0.50	0.32
Southern alpine	0.23	0.53
Northern alpine	-0.13	0.07
Northern lowlands	-1.08	0.35
Eastern lowlands	-0.18	0.79
Total	-0.34	0.53

Table A.2: Slope and p-value of the interpolating linear line of SCA 3 weeks before a peak in discharge in the winter period 2001-2022

– *Delta SCA 3-1 weeks before Qmax over time (winter):*

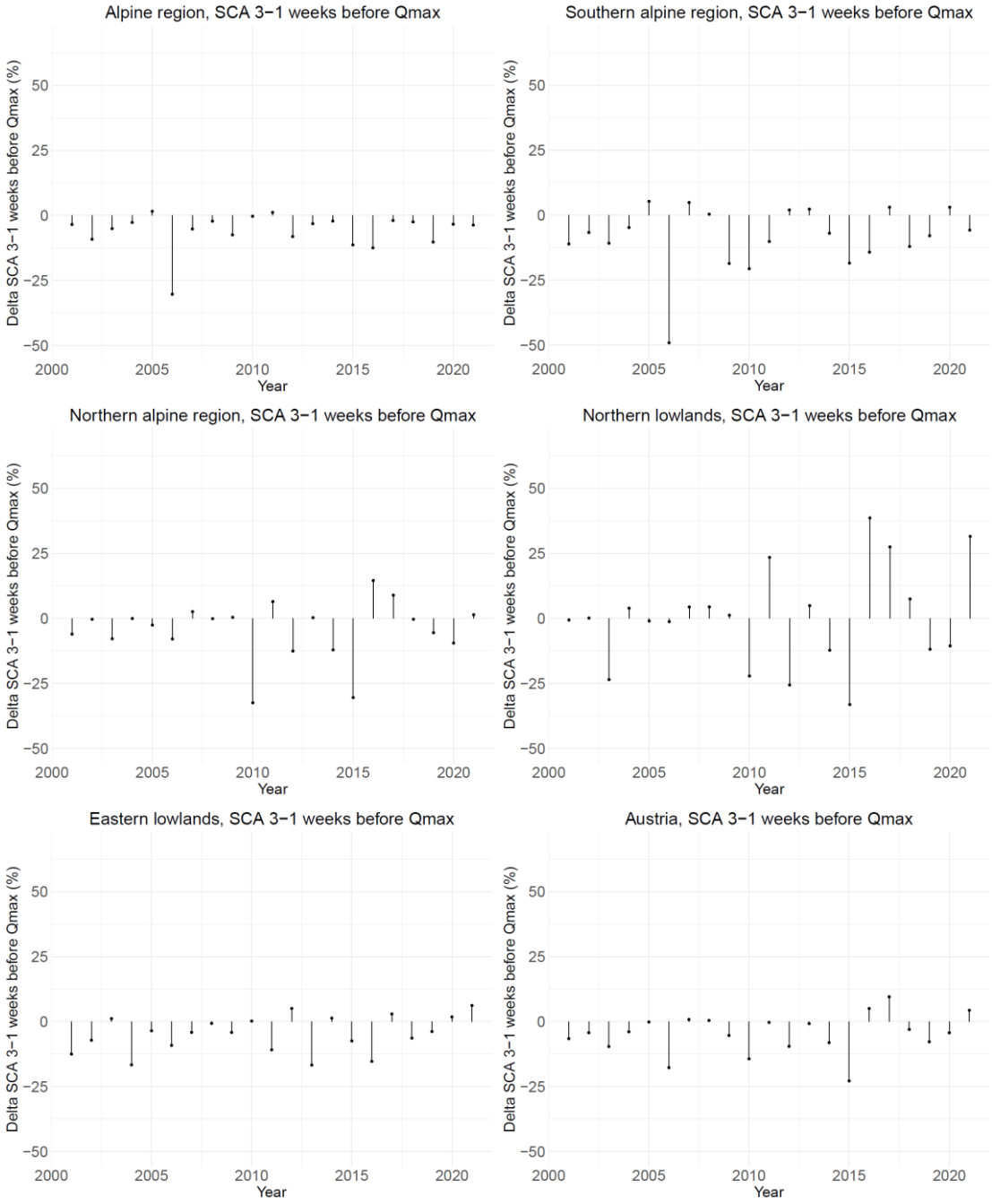

Figure A.2.3: Difference between the values of Snow-Covered Area the third and the first week before the event of maximum in discharge is registered in the winter season, from 2001 to 2022

Regions	Slope of Delta SCA 3-1 weeks (%/year)	Mann-Kendall test, p-value
Alpine	0.07	0.88
Southern alpine	0.29	0.61
Northern alpine	0.05	0.65
Northern lowlands	0.67	0.29
Eastern lowlands	0.36	0.09
Total	0.25	0.38

Table A.3: Difference between the values of snow-covered area the third and first week before the event of maximum in discharge is registered in the winter season, from 2001 to 2022

– *SCA 2 weeks before Qmax over time (spring):*

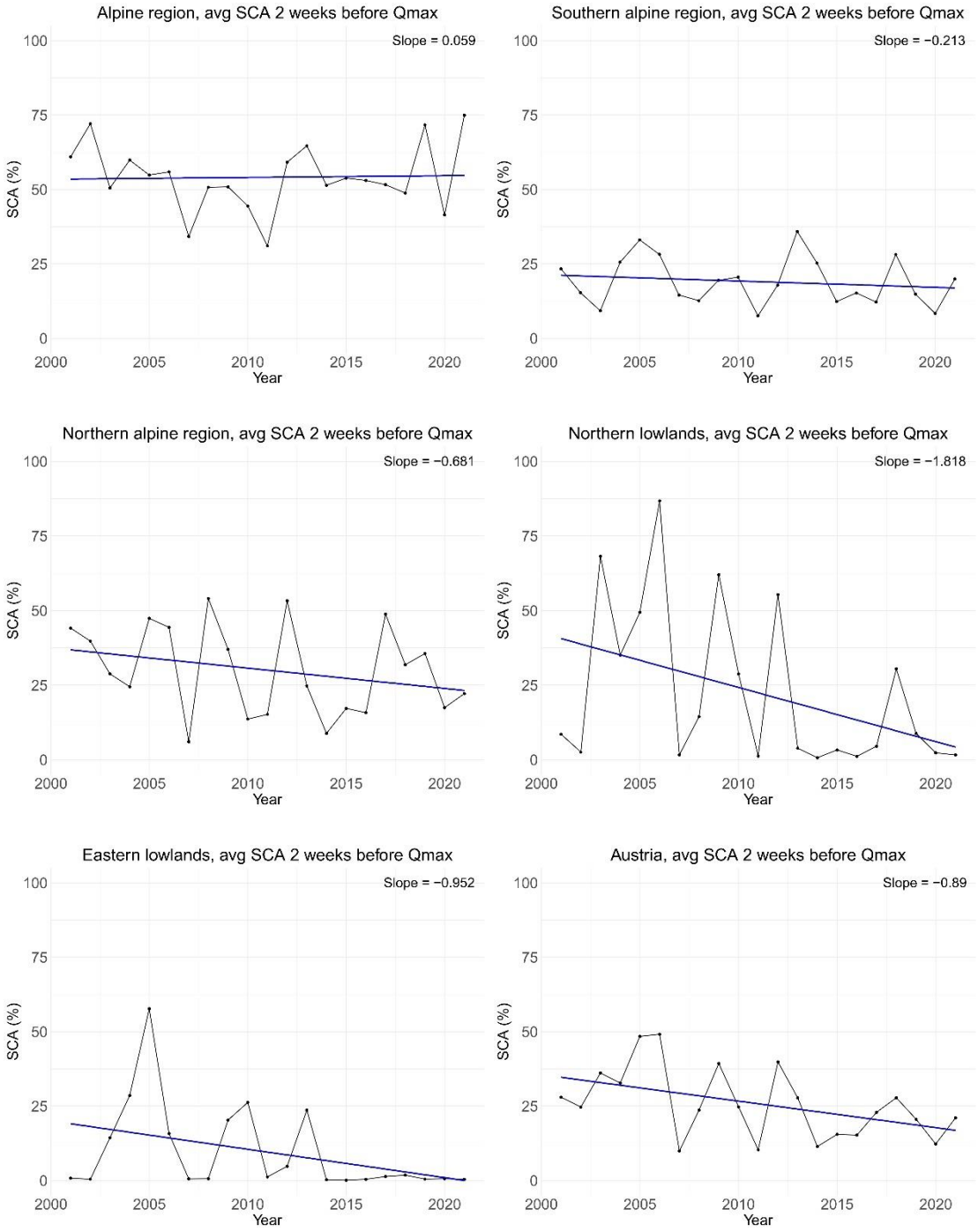

Figure A.2.4: Averaged Snow-Covered Area from the twenty first to the fourteenth day before the event of maximum in discharge registered in the winter season, from 2001 to 2022

Regions	Slope of SCA 2 weeks (%/year)	Mann-Kendall test, p-value
Alpine	0.06	0.74
Southern alpine	-0.21	0.38
Northern alpine	-0.68	0.38
Northern lowlands	-1.82	0.07
Eastern lowlands	-0.95	0.09
Total	-0.89	0.08

Table A.4: Slope and p-value of the interpolating linear line of SCA 2 weeks before a peak in discharge in the spring period 2001-2022

– *SCA 3 weeks before Qmax over time (spring):*

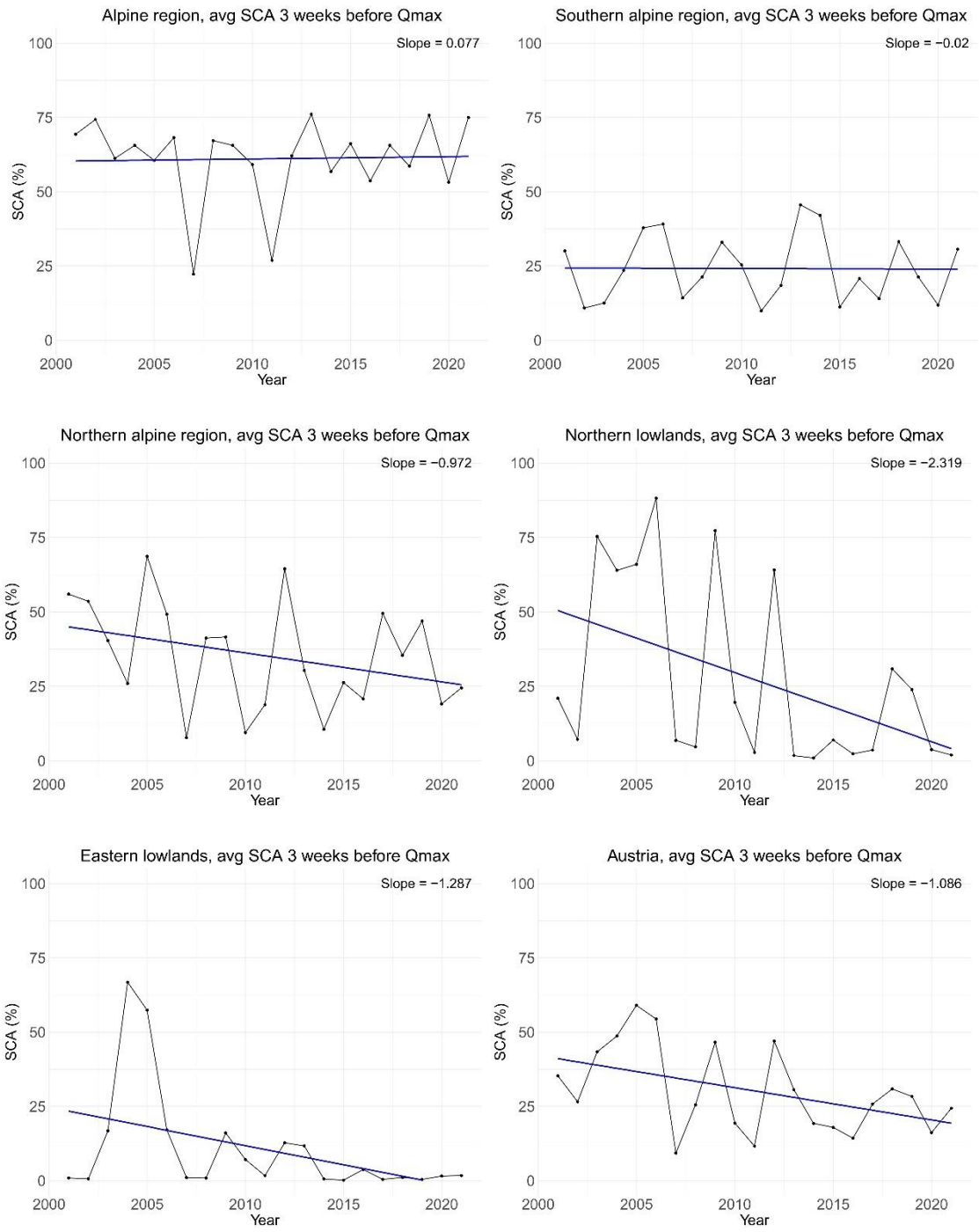

Figure A.2.5: Averaged Snow-Covered Area from the twenty first to the fourteenth day before the event of maximum in discharge registered in the spring season, from 2001 to 2022

Regions	Slope of SCA 3 week (%/year)	Mann-Kendall test, p-value
Alpine	0.08	0.49
Southern alpine	-0.02	0.97
Northern alpine	-0.97	0.19
Northern lowlands	-2.32	0.03
Eastern lowlands	-1.29	0.07
Total	-1.09	0.08

Table A.5: Slope and p-value of the interpolating linear line of SCA 3 weeks before a peak in discharge in the spring period 2001-2022

– *Delta SCA 3-1 weeks before Qmax over time (winter):*

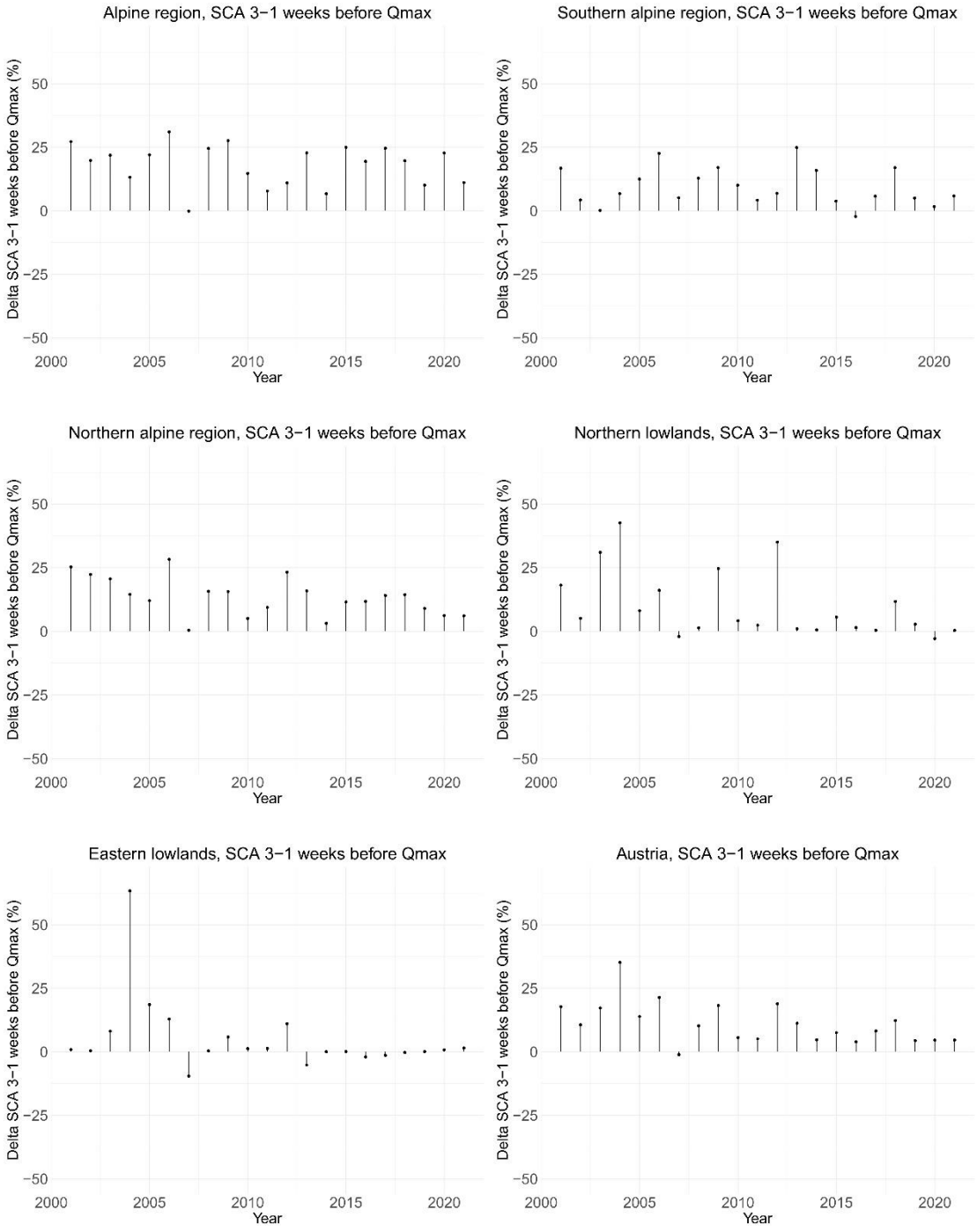

Figure A.2.6: Difference between the values of Snow-Covered Area the third and the first week before the event of maximum in discharge is registered in the spring season, from 2001 to 2022

Regions	Slope of Delta SCA 3-1 weeks (%/year)	Mann-Kendall test, p-value
Alpine	-0.25	0.41
Southern alpine	-0.22	0.45
Northern alpine	-0.62	0.01
Northern lowlands	-1.04	0.01
Eastern lowlands	-0.87	0.11
Total	-0.72	0.01

Table A.6: Difference between the values of snow-covered area the third and first week before the event of maximum in discharge is registered in the spring season, from 2001 to 2022

A.3 Behaviour of correlation values with Area and Elevation

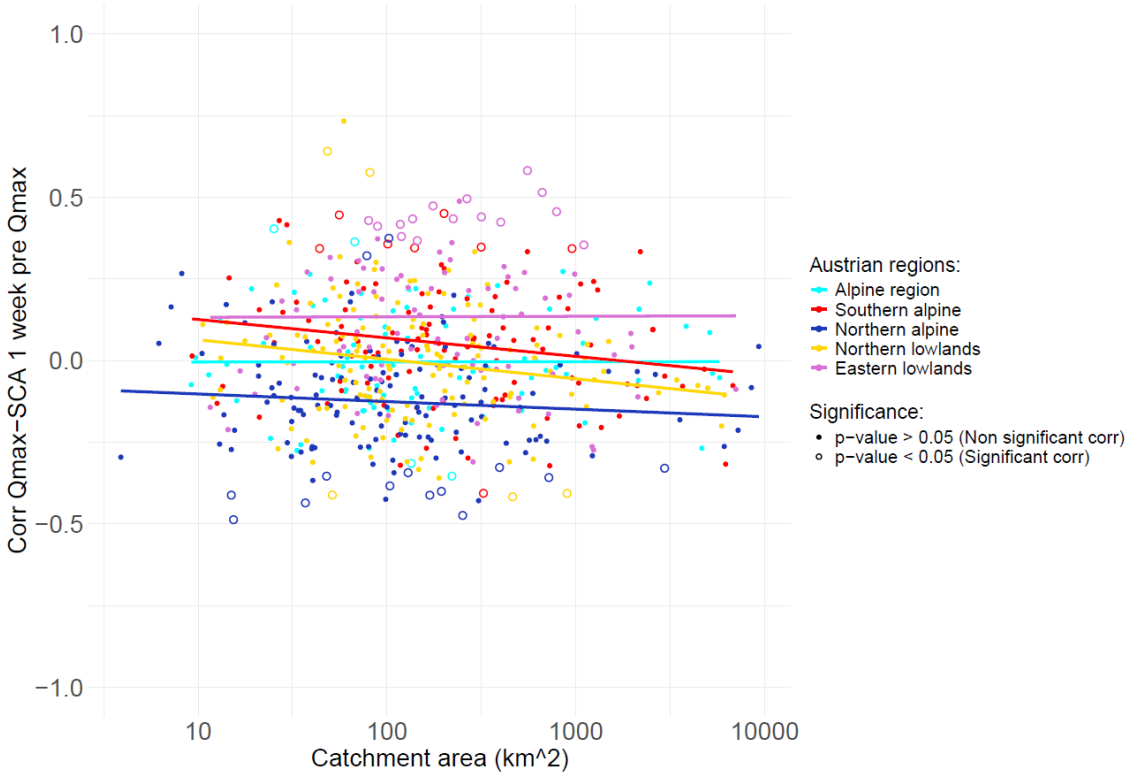

Figure A.3.1: Winter correlation between peak in discharge and average SCA one week before maximum in discharge, in relation to the area of the catchments in the five Austrian regions

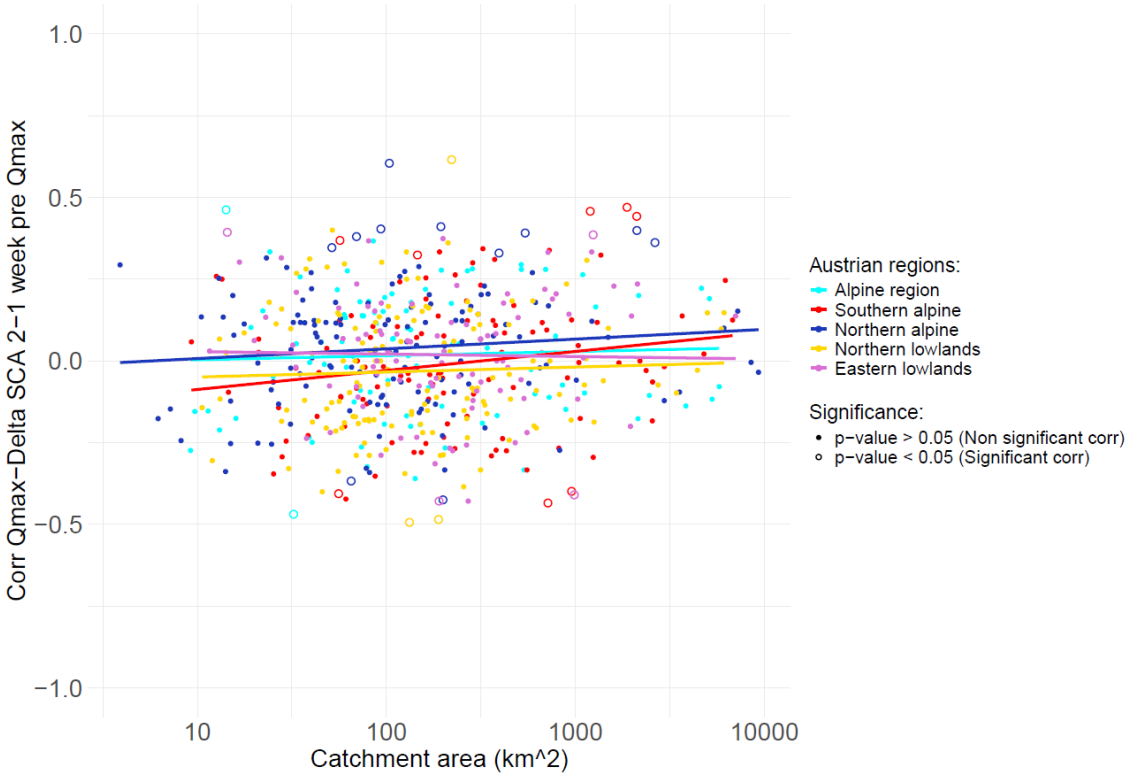

Figure A.3.2: Winter correlation between peak in discharge and difference in SCA the two weeks before a maximum in discharge, in relation to the area of the catchments in the five Austrian regions

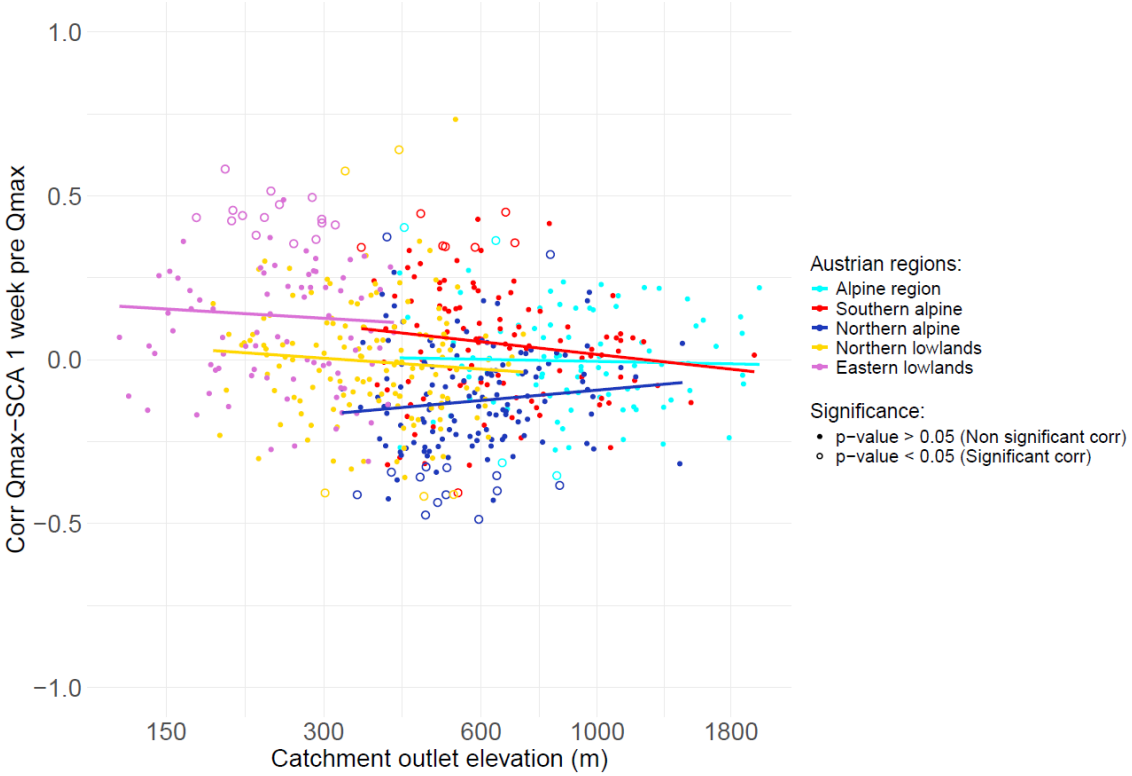

Figure A.3.3: Winter correlation between peak in discharge and average SCA one week before a maximum in discharge, in relation to the elevation of the catchments in the five Austrian regions

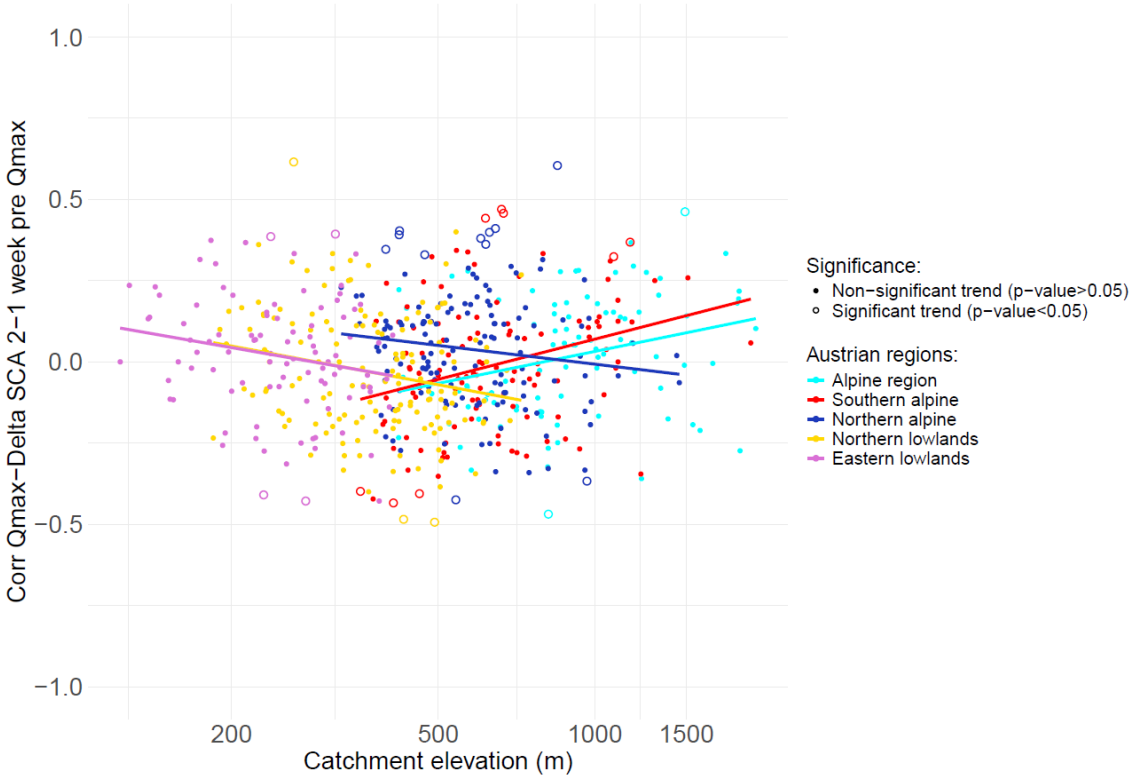

Figure A.3.4: Winter correlation between peak in discharge and difference in SCA the two weeks before a maximum in discharge, in relation to the elevation of the catchments in the five Austrian regions

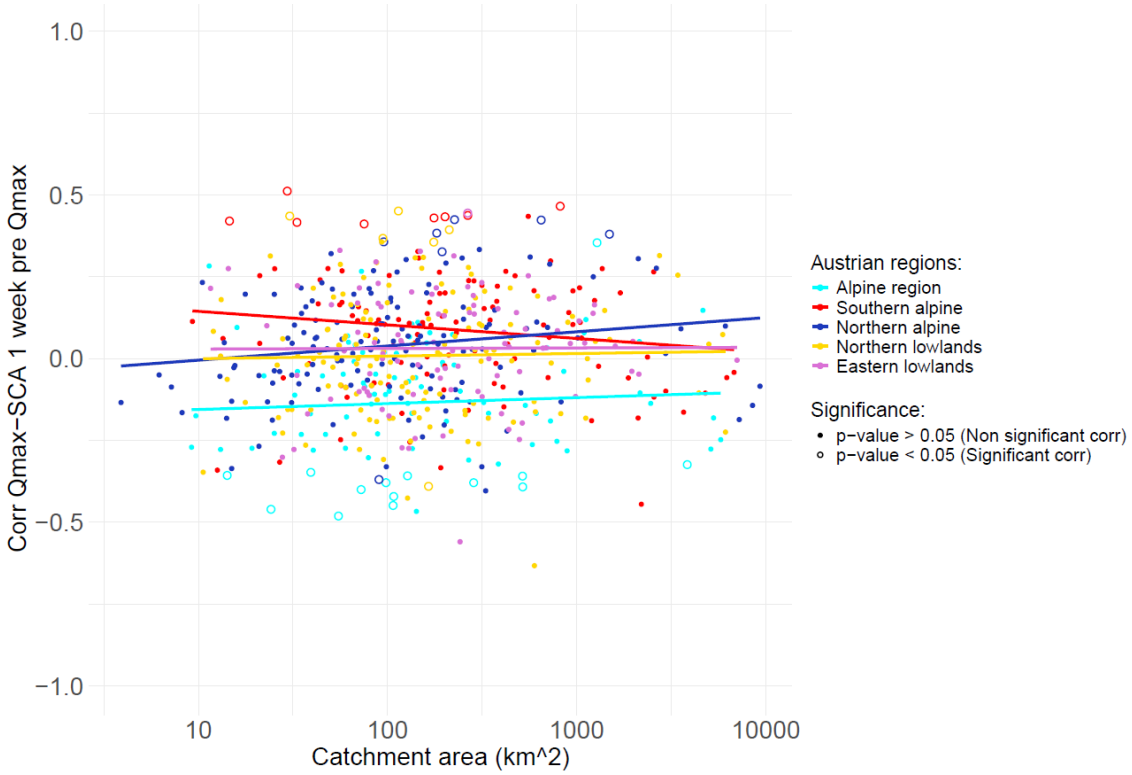

Figure A.3.5: Spring correlation between peak in discharge and average SCA one week before maximum in discharge, in relation to the area of the catchments in the five Austrian regions

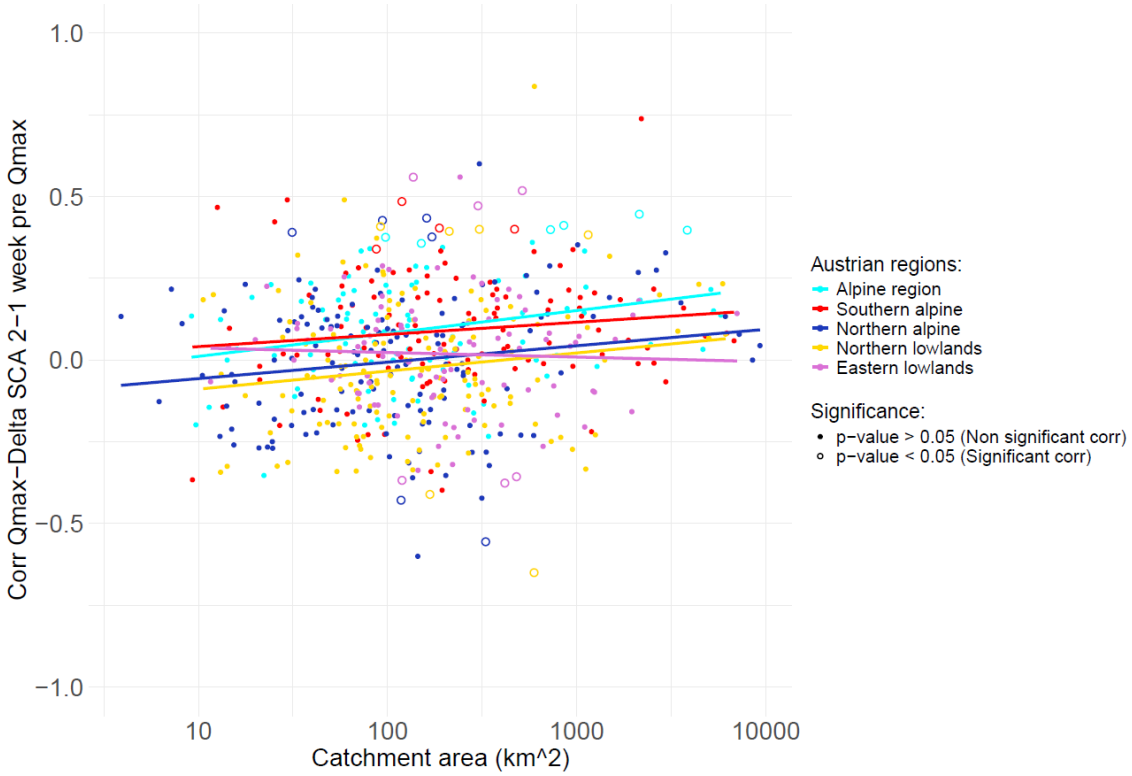

Figure A.3.6: Spring correlation between peak in discharge and difference in SCA the two weeks before a maximum in discharge, in relation to the area of the catchments in the five Austrian regions

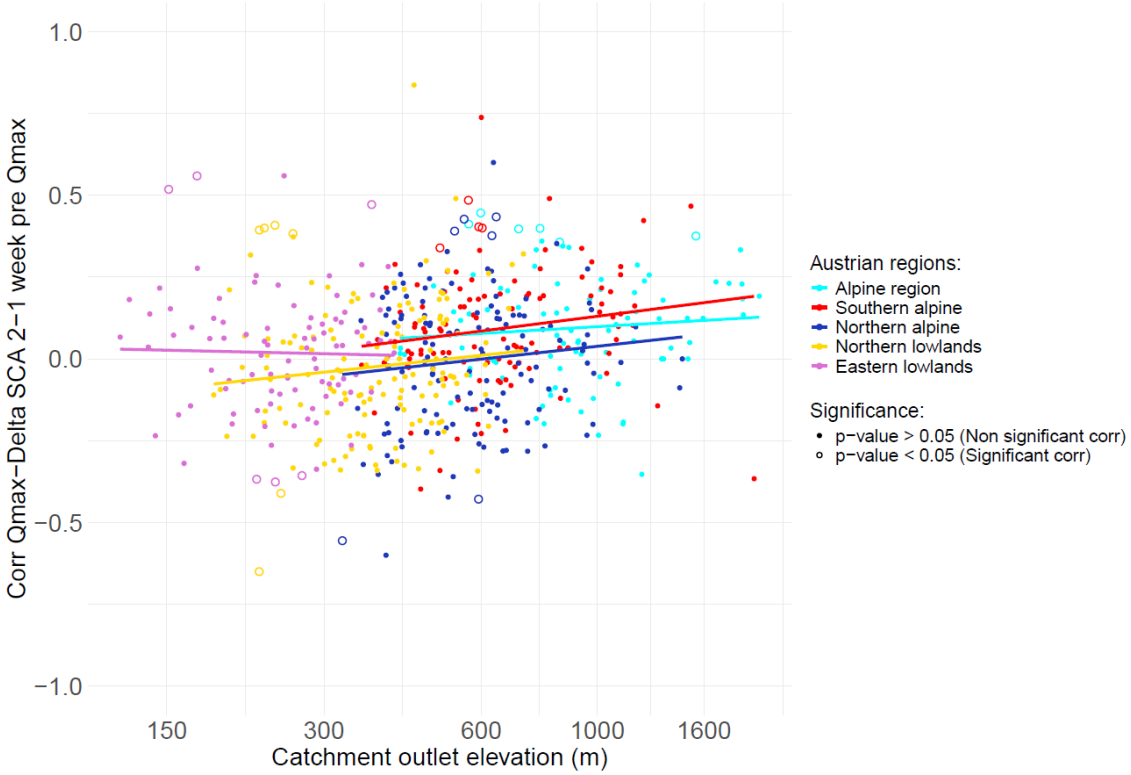

Figure A.3.7: Spring correlation between peak in discharge and difference in SCA the two weeks before a maximum in discharge, in relation to the elevation of the catchments in the five Austrian regions

References

Barnes, W.L., Pagano, T.S., Salomonson, V.V. (1998). Prelaunch characteristics of the moderate resolution imaging spectroradiometer (MODIS) on EOS-AM1. IEEE Transactions on Geoscience and Remote Sensing 36 (4), 1088–1100, doi: 10.1109/36.700993.

Bertola, M., Viglione, A., Vorogushyn, S., Lun, D., Merz, B., & Blöschl, G. (2021). Do small and large floods have the same drivers of change? A regional attribution analysis in Europe. Hydrology and Earth System Sciences, 25(3), 1347–1364, https://doi.org/10.5194/hess-25-1347-2021.

Blöschl, G., Hall, J., Parajka, J., et al. (2017). Changing climate shifts timing of European floods, Science, 357, 6351, 588-590, doi: 10.1126/science.aan2506.

Blöschl, G., et al. (2019a). Twenty-three unsolved problems in hydrology (UPH)–a community perspective. Hydrological Sciences Journal, 64(10), 1141–1158, https://doi.org/10.1080/02626667.2019.1620507.

Blöschl G., Hall J., Viglione A., et al. (2019b). Changing climate both increases and decreases European river floods, Nature,10, https://doi.org/10.1038/s41586-019-1495-6.

Cohen, J., Ye, H., Jones, J. (2015). Trends and variability in rain-on-snow events. 660 Geophysical Research Letters, 42(17), 7115-7122, doi: 10.1002/2015GL065320.

Coles, A.E., McDonnell, J.J. (2018) Fill and spill drives runoff connectivity over frozen ground, Journal of Hydrology, Volume 558, 2018, Pages 115-128, doi: 10.1016/j.jhydrol.2018.01.016.

Gaál, L., Szolgay, J., Kohnová, S., Parajka, P., Merz, R., Viglione, A., and Günter Blöschl (2012). Flood timescales: Understanding the interplay of climate and catchment processes through comparative hydrology, Water Resour. Res., W04511, doi:10.1029/2011WR011509.

Garvelmann, J., Pohl, S., & Weiler, M. (2015). Spatio-temporal controls of snowmelt and runoff generation during rain-on-snow events in a mid-latitude mountain catchment. Hydrological Processes, 29(17), 3649– 3664, doi: 10.1002/hyp.10460.

Haleakala, K., Brandt, W. T., Hatchett, B. J., Li, D., Lettenmaier, D. P., & Gebremichael, M. (2023). Watershed memory amplified the Oroville rain-on-snow flood of February 2017. PNAS Nexus, 2(1), pgac295, https://doi.org/10.1093/pnasnexus/pgac295.

Hall, D.K., Riggs, G.A. (2007). Accuracy assessment of the MODIS snow products. Hydrol. Process. 21, 1534–1547. https://doi.org/10.1002/hyp.6715.

Hirashima, H., Avanzi, F., and Yamaguchi, S. (2017) Liquid water infiltration into a layered snowpack: evaluation of a 3-D water transport model with laboratory experiments, Hydrol. Earth Syst. Sci., 21, 5503–5515, doi: 10.5194/hess-21-5503-2017.

Hundecha, Y., Parajka, J., Viglione A. (2020) Assessment of past flood changes across Europe based on flood-generating processes, Hydrological Sciences Journal, doi: 10.1080/02626667.2020.1782413.

Kemter, M., Merz, B., Marwan, N., Vorogushyn, S., & Blöschl, G. (2020). Joint trends in flood magnitudes and spatial extents across Europe. Geophysical Research Letters, 47, e2020GL087464, doi: 10.1029/2020GL087464.

Madsen, H., Lawrence, D., Lang, M., Martinkova, M., and Kjeldsen, T. R. (2014). Review of trend analysis and climate change projections of extreme precipitation and floods in Europe, J. Hydrol., 519, 3634–3650, https://doi.org/10.1016/j.jhydrol.2014.11.003.

Merz, R., and Blöschl, G. (2003). A process typology of regional floods, Water Resour. Res., 39, 1340, https://doi.org/10.1029/2002WR001952.

Merz, R. and Blöschl, G. (2008). Flood frequency hydrology: 1. Temporal, spatial, and causal expansion of information, Water Resour. Res., 44, W08432, https://doi.org/10.1029/2007WR006744.

Merz, R., and Blöschl, G. (2009). A regional analysis of event runoff coefficients with respect to climate and catchment characteristics in Austria, Water Resour. Res., Vol. 45, W01405, doi:10.1029/2008WR007163.

Paudel, K.P., Andersen, P. (2011). Monitoring snow cover variability in an agropastoral area in the Trans Himalayan region of Nepal using MODIS data with improved cloud removal methodology. Remote Sens. Environ., 115, 5, 1234–1246, doi: 10.1016/j.rse.2011.01.006.

Parajka, J., Blöschl, G. (2008). Spatio-temporal combination of MODIS images – potential for snow cover mapping. Water Resour. Res. 44 (3). https://doi.org/10.1029/2007WR006204.

Parajka, J., Blöschl, G. (2008). The value of MODIS snow cover data in validating and calibrating conceptual hydrologic models, Journal of Hydrology 358, 240-258, https://doi.org/10.1016/j.jhydrol.2008.06.006.

Parajka, J., Blöschl, G. (2006). Validation of MODIS snow cover images over Austria. Hydrol. Earth Syst. Sci. 10 (5), 679–689. https://doi.org/10.5194/hess-10-679-2006.

Parajka, J., Blöschl, G. (2012). MODIS-based snow cover products, validation, and hydrologic applications. In: Chang, N.B., Hong, Y. (Eds.): Multiscale Hydrologic Remote Sensing: Perspectives and Applications. CRC Press, Taylor & Francis Group, Boca Raton, pp. 185–212, ISBN 1000687279, 9781000687279.

Parajka, J., Holko, L., Kostka, Z., Blöschl, G. (2012). MODIS snow cover mapping accuracy in a small mountain catchment–comparison between open and forest sites. Hydrol. Earth Syst. Sci. 16, 2365–2377. https://doi.org/10.5194/hess-16-2365-2012.

Schöner, W., Koch, R., Reisenhofer, S., Strasser, U., Marke, T., Marty, C., Tilg, A. (2016): Snow in Austria during the instrumental period - spatiotemporal patterns and their causes - relevance for future snow scenarios, Endbericht ACRP Projekt Snowpat, 43 pp.

Tong, R., Parajka, J., Komma, J., Blöschl, G. (2020), Mapping snow cover from daily Collection 6 MODIS products over Austria, Journal of Hydrology, Volume 590, November 2020, 125548, https://doi.org/10.1016/j.jhydrol.2020.125548.

Wang, W., Huang, X., Deng, J., Xie, H., Liang, T. (2015). Spatio-temporal change of snow cover and its response to climate over the Tibetan plateau based on an improved daily cloud-free snow cover product. Remote Sens., 7, 1, 169–194, doi: 10.3390/rs70100169.